

# **The Fabrication of Copper Sulfide-Based Electrochemical Sensors**

By

Benjamin Cheung

A Thesis

Submitted for the Partial Fulfillment of the Requirements for

the Degree of B. Sc. Honors Biochemistry with Thesis

Department of Chemistry and Biochemistry

University of Windsor

Windsor, Ontario, Canada

By: Benjamin Cheung

© 2019 Benjamin Cheung

## **Declaration of Originality**

I hereby certify that I am the sole author of this thesis and that no part of this thesis has been published or submitted for publication.

I certify that, to the best of my knowledge, my thesis does not infringe upon anyone's copyright nor violate any proprietary rights and that any ideas, techniques, quotations, or any other material from the work of other people included in my thesis, published or otherwise, are fully acknowledged in accordance with the standard referencing practices. Furthermore, to the extent that I have included copyrighted material that surpasses the bounds of fair dealing within the meaning of the Canada Copyright Act, I certify that I have obtained a written permission from the copyright owner(s) to include such material(s) in my thesis and have included copies of such copyright clearances to my appendix.

I declare that this is a true copy of my thesis, including any final revisions, as approved by my thesis committee and that this thesis has not been submitted for a higher degree to any other University or Institution.

## **Acknowledgements**

The completion of this project was made possible thanks to the supervision and guidance of Dr. Jichang Wang. It was an honour to be a member in your research group, and I have gained many valuable lessons from this experience.

I would also like to thank the rest of the Wang Research group – Alexander Tang, Michelle Dao, and Xin Zeng for their assistance and support throughout this project. In addition, I would like to thank Dr. S. Holger Eichhorn for accepting to become my reader and taking the time to review this work. I would also like to thank Dr. Robert Schurko for being the course instructor.

## Abstract

In this research, a novel electrochemical approach on the basis of oscillatory oxidation of sodium bisulfite was developed to prepare copper sulfide nanoparticles. The three-electrode system utilized glassy carbon, Ag/AgCl, and copper wire as the working, reference and counter electrodes, in which the copper sulfide particles were formed at the counter electrode. Characterization of the modified copper sulfide electrode with scanning electron microscopy and energy dispersive x-ray spectroscopy validate the formation of copper sulfide and illustrate that both the particle size and morphology can be conveniently manipulated by adjusting the length of the copper counter electrode. The as-prepared copper sulfide coated electrodes exhibit strong catalytic activity towards the electro-oxidation of glucose and are stable in air for a period eight of days, making it a promising candidate as an electrochemical sensor.

Using the activity towards glucose oxidation as a reference, this research optimized the applied potential, the concentration of bisulfite, and the length of the copper counter electrode for synthesizing copper sulfide particles with the highest electrocatalytic activity. Preliminary characterization with cyclic voltammetry suggests that the oxidation of glucose at the copper sulfide electrode surface is diffusion-controlled. The anodic peak current is found to change linearly with respect to glucose concentration over a broad range.

## Table of Contents

<b>Declaration of Originality</b>	ii
<b>Acknowledgements</b>	iii
<b>Abstract</b>	1
<b>Table of Contents</b>	2
<b>List of Figures</b>	4
<b>List of Abbreviations</b>	8
<b>Chapter 1: Introduction</b>	9
1.1 Electrochemical Sensors.....	9
1.2 Chalcogenides.....	14
1.2.1 Copper Sulfide	16
1.3 Methods of Synthesizing Copper Sulfide.....	18
1.4 Electrochemical Oscillations.....	20
<b>Chapter 2: Project Overview</b>	24
2.1 Research Objectives.....	24
2.2 Experimental Methods.....	24
<b>Chapter 3: Results and Discussion</b>	27
3.1 Fabrication of the Copper Sulfide Sensor on the Counter Electrode.....	27
3.1.1 Analysis of Oscillatory Behavior	31
3.1.2 Proposed Mechanism of the Formation of Copper Sulfide	35
3.2 Imaging the Electrode Surface.....	37
3.3 Fabrication Optimization.....	40
3.3.1 Investigating the Effects of the Applied Potential	40
3.3.2 Optimizing Sodium Bisulfite Concentration	45
3.3.3 Optimizing the Length of the Counter Electrode	49
3.4 Detection of D-(+)-Glucose.....	58
3.4.1 Qualitative and Quantitative Detection	58
3.4.2 Mechanism of Glucose Oxidation	62
3.4.3 Stability	65

<b>Chapter 4: Conclusions</b>	67
<b>Chapter 5: Future Directions</b>	69
<b>References</b>	70
<b>Vita Auctoris</b>	73

## List of Figures

<b>Figure 1:</b> Schematic of a three electrode setup.	11
<b>Figure 2:</b> Cyclic voltammogram showing the direction in which the potential was scanned and the oxidation and reduction peak. <sup>7</sup>	12
<b>Figure 3:</b> Transmission electron micrographs of CuS with different morphologies: (a) nanospheres, (b) hollow nanospheres, (c) hexagonal nanoplates, and (d) nanorods. <sup>16</sup>	17
<b>Figure 4:</b> Schematic of the steps in cathodic deposition of metals. <sup>22</sup>	19
<b>Figure 5:</b> Schematic shape of the Nyquist diagrams for the systems: (a) N-NDR region; (b) hidden NDR region; and (c) S-NDR region. <sup>27</sup>	22
<b>Figure 6:</b> Comparison of I-E dependencies for the (a) N-shaped and (b) S-shaped NDR characteristics. <sup>27</sup>	23
<b>Figure 7:</b> Four electrode system for fabrication of the modified electrode via potentiostatic reaction.	25
<b>Figure 8:</b> Three electrode system for the detection via cyclic voltammetry (the same as Figure 1).	26
<b>Figure 9:</b> Potentiostatic time series of the fabrication of a modified copper wire electrode.	27
<b>Figure 10:</b> Time series of the potential of the counter electrode recorded during the fabrication of a CuS nanoparticles.	28
<b>Figure 11:</b> A series of CVs that compare the various modified copper wires with varying times of fabrication.	30
<b>Figure 12:</b> Comparison of the potentiostatic time series at the GCE and the time series of the potential value at the counter for the time interval of 0 to 100 seconds.	31

<b>Figure 13:</b> Comparison of the potentiostatic time series at the GCE and the time series of the potential value at the counter for the time interval of 400 to 500 seconds.	33
<b>Figure 14:</b> SEM Images at 5000x magnification showing the morphology of the modified copper counter electrode for (a) 1.5cm length and (b) 0.5cm length in 0.3M sodium bisulfite concentration.	38
<b>Figure 15:</b> SEM Images for the modified counter copper sulfide electrode at 5000x magnification for (a) 1.5cm, (b) 1.0cm, and (c) 0.5cm length in 0.5M sodium bisulfite concentration.	38
<b>Figure 16:</b> EDS of the SEM sample shown in Figure 15 (a).	39
<b>Figure 17:</b> Potentiostatic time series at the working electrode during the fabrication of the CuS nanoparticles at various potentials.	41
<b>Figure 18:</b> Time series of the potential of the counter electrode recorded during the fabrication of a CuS nanoparticles at various potentials.	42
<b>Figure 19:</b> CVs of the modified copper electrodes that were prepared with different applied potentials.	43
<b>Figure 20:</b> Potentiostatic time series of the fabrication of the modified counter electrode with varying sodium bisulfite concentration in 0.1M sulfuric acid solution.	45
<b>Figure 21:</b> Time series of the counter electrode potential during the fabrication of the modified counter electrode with varying sodium bisulfite concentration.	46
<b>Figure 22:</b> CVs of the 10th scan of the modified counter electrodes that were fabricated in varying concentrations of sodium bisulfite during potentiostatic experiments.	47
<b>Figure 23:</b> Potentiostatic time series of the fabrication of the modified counter electrode in 0.5M sodium bisulfite concentration at varying lengths.	50

<b>Figure 24:</b> Time series of the potential of the counter electrode recorded during the fabrication of CuS nanoparticles for various lengths in 0.5M bisulfite concentration.	51
<b>Figure 25:</b> CVs of the 10th scan of the modified counter electrodes that were fabricated at various lengths during potentiostatic experiments. Each modified electrode was restricted a length of 0.5cm prior to detection with cyclic voltammetry.	52
<b>Figure 26:</b> Potentiostatic time series of the fabrication of the modified counter electrode in 0.3M sodium bisulfite concentration and 0.1M sulfuric acid concentration varying lengths.	53
<b>Figure 27:</b> Time series of the potential of the counter electrode recorded during the fabrication of a CuS nanoparticles in 0.3M sodium bisulfite concentration.	54
<b>Figure 28:</b> CVs of the 10th scan of the modified counter electrodes that were fabricated at varying lengths.	55
<b>Figure 29:</b> Images of the modified copper sulfide electrodes of Figure 26 and 27. A is 1.5cm, B is 1.0cm, C is 0.75cm, and D is 0.50cm. Each modified electrode was restricted to a length of 0.50cm following the fabrication.	56
<b>Figure 30:</b> CVs of the 10th scan for the modified and unmodified copper electrodes.	59
<b>Figure 31:</b> CVs of the 10th scan for the modified electrodes in increasing glucose concentration with a scan rate of 100mV/sec. Each electrode was restricted to a length of 1.0cm.	60
<b>Figure 32:</b> Calibration curve of the peak current plotted as a function of the concentration in glucose (mM) during CV using the modified copper sulfide electrode. Data taken from the CVs of the 10th scan for the modified electrodes in increasing glucose concentration.	61

**Figure 33:** A series of CVs at different scan rates. The solution contains 0.5mM glucose and 0.1M NaOH. The modified copper sulfide electrode was fabricated in 0.3M sodium bisulfite and 0.1M sulfuric acid solution for 1200 seconds with a length of 1.0cm. 62

**Figure 34:** Peak current plotted as a function of the square root of the scan rate. The reactions were conducted in a 0.5mM glucose and 0.1M NaOH solution. 64

**Figure 35:** A series of CVs of a modified copper sulfide electrode that were fabricated in 0.3M sodium bisulfite and 0.1M sulfuric acid with a length of 1.0cm at 1500mV potential for 1200 seconds. 65

### **List of Abbreviations**

Ag/AgCl – Silver/Silver Chloride

CMPDR – Capacitance Mediated Positive Differential Resistance

CV – Cyclic Voltammetry

ddH<sub>2</sub>O – Double Distilled Water

EDS - Energy-dispersive X-ray spectroscopy

GCE – Glassy Carbon Electrode

HN-NDR – Hidden Negative Differential Resistance

LOD – Limit of Detection

NDR - Negative Differential Resistance

N-NDR – N-shaped Negative Differential Resistance

SEM – Scanning Electron Microscopy

S-NDR – S- shaped Negative Differential Resistance

## Chapter 1: Introduction

### 1.1 Electrochemical Sensors

Electrochemical sensors are devices which provide information about the composition of a system in real time. It is done by coupling a chemically selective layer which is known as the recognition element to an electrochemical transducer.<sup>1</sup> The selective interaction between the sensor and the chemical species is transduced into an analytically useful signal.<sup>1</sup> Electrochemical sensors are attracting great interest as it is simple to miniaturize and integrate them into automatic systems without compromising analytical characteristics.<sup>1</sup> Due to their selectivity and sensitivity as well as their low cost, electrochemical sensors have become a valuable tool in a variety of disciplines with applications in physical chemistry, materials science, biochemistry, environmental analysis, and solid-state physics.<sup>2</sup>

Stability, activity, and selectivity are factors which are of great importance in electrochemical sensing.<sup>2</sup> Stability refers to the time period in which it can produce reproducible results. Activity refers to how reactive the sensor is to the analyte of interest. Selectivity refers to the sensor's ability to measure the analyte of interest in the presence of other interfering species. Low cost, miniaturization, and reproducibility must also be considered when developing new electrochemical sensors.<sup>2</sup>

There are three main types of electrochemical techniques involved in the application of electrochemical sensors: potentiometric, amperometric, and conductometric.<sup>3</sup> Potentiometric electrochemical sensors are capable of selectively measuring and quantifying a particular species. In potentiometric sensors, the potential difference between the working electrode and reference electrode is measured under

conditions of no current flow.<sup>4</sup> They are constructed by the preparation of a membrane which is permselective for a particular ion, and thereby, develops a membrane potential in contact with a solution of the analyte ion.<sup>1</sup> The electrodes built up with these membranes are called ion selective electrodes and a well-known example would be the glass electrode for pH measurements.<sup>1</sup> Potentiometric sensors work by having a reference electrode at a constant activity while the other electrode is the working electrode whose potential is determined by its environment. Since the potential of the reference electrode is constant, the value of the potential difference can be related to the concentration of the reagents to be detected.<sup>3</sup>

In amperometric and voltammetric measurements, the current measurement in amperes is involved and potentials of the electrode are held constant or used as a variable input during measurements.<sup>4</sup> Amperometry is a method which utilizes amperometric sensors in order to monitor the reduction or oxidation of the analytes in the presence of a fixed potential by measuring the changes in current.<sup>5</sup> A working potential is applied for a short duration while the current is measured. Chronoamperometry is a time-dependent technique in which a fixed potential is applied to the working electrode and the resulting current is monitored as a function of time.

In voltammetric sensors, the current response is measured as a function of applied potential. The potential is varied step by step or continuously in order to determine the current as a function of the cell's potential. As shown in Figure 1, a three electrode setup is typically utilized for a voltammetric sensor which consists of a working, auxiliary, and reference electrode. The reference electrode acts as a reference in measuring and stabilizing the potential of the working electrode. The working electrode

is the electrode at which the oxidation or reduction usually being investigated takes place. The auxiliary or counter electrode completes the circuit and is made of a conductive material. The electron transfer reaction of the analytes is driven by the applied potential.<sup>4</sup> In the electrochemical cell, a supporting electrolyte is necessary to allow the system to be less resistant to the movement of charge and to maintain constant ionic strength.<sup>3</sup> The measured current directly indicates the rate of the electron transfer in an electrochemical reaction.<sup>4</sup>

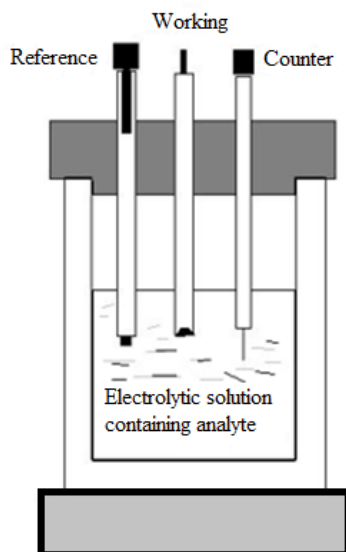


**Figure 1:** Schematic of a three electrode setup.

Cyclic voltammetry (CV) is a technique used for voltammetric electrochemical sensing. The response in a current is recorded while a potential scan is applied to the working electrode at a constant scan rate. It is commonly employed to investigate the reduction and oxidation processes of molecular species in order to determine its detection capabilities. The potential applied to the working electrode increases and decreases as it is cycled through the predetermined potential range.<sup>6</sup> A cyclic voltammogram is obtained

by measuring the current at the working electrode during the potential scan in which the current response is plotted as a function of the applied potential.<sup>6</sup> As shown in Figure 2, a typical cyclic voltammogram has the applied potential on the x-axis plotted against the current on the y-axis. The arrow typically indicates the direction in which the potential was scanned to record the data. In cyclic voltammograms, the scan rate will be stated which indicates the speed in which the potential was varied linearly at per second.<sup>7</sup> The concentration of the analyte in the solution is typically proportional to the detected value for the current.<sup>7</sup>

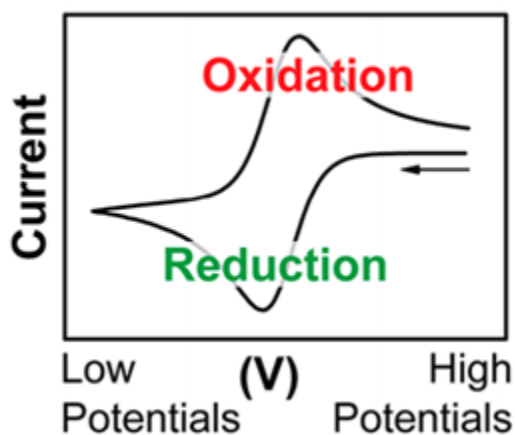


**Figure 2:** Cyclic voltammogram showing the direction in which the potential was scanned and the oxidation and reduction peak.<sup>7</sup>

Conductometric sensors are based on conductive or semi conductive materials which change their conductivity upon interaction with a chemical species.<sup>4</sup> The sensing material which is specific to the analyte in question is sandwiched between two contact electrodes and the resistance of the entire device is measured.<sup>4</sup> It is composed of two basic components which consists of the electrodes and a sensitive layer.<sup>4</sup> The resistance between the two sensing electrodes changes when the sensing layer comes into contact

with the specific analyte.<sup>4</sup> It is low cost and simple which is attractive as no reference electrodes are necessary.<sup>3</sup> Conductometric sensors are fundamentally non selective, however, they can be modified in order to increase sensitivity.<sup>3</sup> Typically, these sensors are mostly utilized as gas sensors due to their conductivity changes following surface chemisorption.<sup>3</sup> A common example of a conductometric sensor is the alcohol breathalyzer which is utilized to test the blood alcohol levels of drivers.<sup>8</sup>

The performance of electrochemical sensors are influenced heavily by the working electrode material. Excellent working electrodes have better signal-to-background characteristics and provide reproducible results.<sup>3</sup> Popular working electrodes include various forms of carbon, platinum, gold, silver, and copper due to their versatile potential window, low background current, chemical inertness, and low cost.<sup>3</sup> Electrochemical sensors also allow for the ability to modify the surface of the working electrode through chemical and electrochemical methods. These surface modifications grant properties to the working electrode such as improved selectivity, sensitivity, and/or stability.<sup>9</sup> Due to the ability to modify the surface of the working electrode, the properties and reactivity of the electrode can be controlled which allows for further applications like in biosensors.<sup>3</sup>

## 1.2 Chalcogenides

Over the past decades, transition metal chalcogenides have attracted ever-growing research interests as potential electrode materials for energy storage and conversion due to its unique crystal structures, rich redox sites, tunable stoichiometric compositions, and relatively higher electrical conductivity in comparison to their transition metal oxide counterparts.<sup>10</sup> A chalcogenide is a chemical compound containing a chalcogen as the negative ion. The term chalcogen defines all group 16 elements of the periodic table.<sup>11</sup> Chalcogenide is referred to the sulfides, selenides, and tellurides as distinct from their oxides.<sup>11,12</sup> Phases existing in the systems, M-S, M-Se, and M-Te in which M is the transition metal differ considerably from the phases in the system, M-O in regards to their chemical and physical properties as well as structures.<sup>12</sup> These differences originate between the oxygen atom and the atoms of S, Se, and Te.<sup>12</sup> Chalcogen elements differ from the atomic properties of oxygen such that chalcogen atoms are larger and heavier than oxygen atoms. Additionally, they are less electronegative than oxygen and have d orbitals of accessible energy (3d for S, 4d for Se, 5d for Te), which oxygen atoms lack.<sup>12</sup> The differences in the atomic properties result in differences in the bonding of the transition metals to S, Se, and Te relative to the transition metal to oxygen bonding.<sup>12</sup>

As the chalcogens S, Se, and Te have relatively low electronegativity, their bonds with transition metals and post-transition metals will be largely covalent. The covalency is due to the mixing of the valence s and p orbitals of the chalcogen with the outer s and p orbitals of the metal. This results in the formation of a broad valence band and a broad conduction band. The valence band (bonding) is mainly due to the more electronegative species of the elements while the conduction band (antibonding) is due to the metal.<sup>12</sup> In

most chalcogenides of post transition metals, the valence band is occupied completely by electrons, thus, the chalcogen's formal oxidation state is -2. Since the conduction band is empty, these compounds are semiconductors.<sup>12</sup> Their resistance decreases as their temperature increases, which is opposite to that of a metal. By controlled introduction of impurities, their conducting properties may be altered. The semiconductor properties of chalcogenides allow for its utilization in optoelectronic device applications which include transistors, solar cells, and photodetectors.<sup>13</sup>

### 1.2.1 Copper Sulfide

Copper sulfide is a transition metal sulfide which is inexpensive and a naturally abundant functional semiconductor that is available in a variety of different phases such as chalcocite ( $\text{Cu}_2\text{S}$ ), villamaninite ( $\text{CuS}_2$ ), djurleite ( $\text{Cu}_{1.95}\text{S}$ ), anilite ( $\text{Cu}_{1.75}\text{S}$ ), and covellite ( $\text{CuS}$ ).<sup>14</sup>  $\text{CuS}$  is a type of chalcogenide which is utilized in energy and catalysis-related applications such as energy storage and conversion devices, gas sensors, and photocatalysts.<sup>14</sup> An example of such applications would be the research of Liang *et al* who have observed the photocatalytic properties of nanoporous  $\text{CuS}$ .<sup>15</sup>

In  $\text{CuS}$ , complete condensation of the valence-band holes does not take place as only two-thirds of the chalcogenide ions are present as  $\text{X}_2^{2-}$  pairs, while one third remains as isolated  $\text{X}^-$ .<sup>12</sup> Thus,  $\text{CuS}$  is considered a p-type semiconductor. In general, p-type semiconductors can be created by doping an intrinsic semiconductor with an electron acceptor element during the manufacturing process. The electron acceptor dopant is an atom which accepts an electron from the lattice, thus, creating a vacancy where an electron should be which is referred to as a hole. These holes can move through the crystal like a positively charged particle.

$\text{CuS}$  nanoparticles, in particular, have a variety of morphologies which can influence their properties and potential applications.<sup>16</sup>  $\text{CuS}$  nanoparticles are of increasing interest due to their excellent optical and electrical properties. They are gradually emerging as a promising platform for sensing, molecular imaging, photothermal therapy, and drug delivery.<sup>16</sup> The ability to synthesize  $\text{CuS}$  nanoparticles of various morphologies have opened up more diverse applications due to its different functions.<sup>16</sup> As shown in Figure 3, there are a variety of morphologies in regards to  $\text{CuS}$  nanoparticles. Spherical

CuS nanoparticles have found applications in biomedicine, while hollow nanospheres and nanocages hold promising potential in drug delivery.<sup>16</sup> CuS nanorods and nanowires have been successfully utilized for the sensing of small molecules, food pathogens, and immunologically relevant moieties.<sup>16</sup>

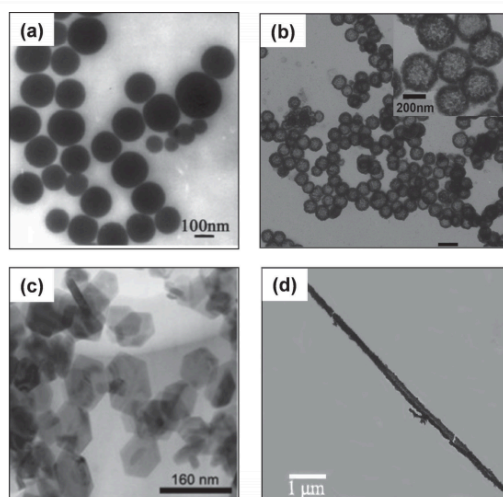


**Figure 3:** Transmission electron micrographs of CuS with different morphologies: (a) nanospheres, (b) hollow nanospheres, (c) hexagonal nanoplates, and (d) nanorods.<sup>16</sup>

### 1.3 Methods of Synthesizing Copper Sulfide

A variety of different approaches have been adopted to synthesize CuS, including solvothermal synthesis, microemulsions, and electrodeposition.<sup>14,16-20</sup> The solvothermal synthesis is a method which is low-cost, low-risk, and easy to operate. It is a synthetic technique which can facilitate and accelerate the reaction among the reactants and tailor the properties of the nanomaterials by varying the reaction parameters.<sup>20</sup> In this method, the reactants are placed into an organic solvent or water.<sup>20</sup> The reaction is carried out under high pressure and temperature conditions. If the reaction medium used are nonaqueous solvents, it is termed as the solvothermal method. It is referred to as the hydrothermal process if the preparation is carried out in the presence of water.<sup>20</sup>

Microemulsions are isotropic, macroscopically homogeneous, and thermodynamically stable solutions containing at least three components: a polar phase, a nonpolar phase, and a surfactant.<sup>21</sup> Different microstructures are formed from the interfacial layer ranging from droplets of oil dispersed in a continuous water phase over a bicontinuous sponge phase to water droplets dispersed in a continuous oil phase.<sup>21</sup> The bicontinuous sponge phase can be used as nanoreactors for the synthesis of nanoparticles.<sup>21</sup>

Electrodeposition is a well-known method to produce in situ metallic coatings by the actions of an electric current on conductive material which is immersed in a solution containing a salt of the metal to be deposited.<sup>22,23</sup> It is inexpensive and does not require harsh conditions. This technique allows for the control of the thickness and morphology of the nanostructure being formed by adjusting the electrochemical parameters.<sup>22,23</sup> The electrodeposition method utilizes an electrolytic cell circuit consisting of an anode, a

cathode, an electrolytic bath, a current source, and an ampere/voltmeter. Reduction and oxidation occur at the cathode and anode, respectively, due to metal ions and electrons which cross the electrode-electrolyte interface.<sup>22</sup> The electrodeposition occurs on the anode or cathode, depending on whether the electrode is oxidized or reduced. In simple salt solutions, metal ions are presented in the bulk solution as hydrated ions. As shown in Figure 4, a number of reactions are involved in the discharge process of ions under the influence of an electric field. In the figure, a cathode is being modified by electrodeposition. The transport of hydrated ions towards the cathode surface is the initial step which is followed by the alignment of water molecules in the diffusion layer. The removal of water molecules in the Helmholtz layer occurs as the next step. Adsorption of the ions at the cathode surface are referred to as “adatoms”. These adatoms are discharged and neutralized. It is followed by the surface diffusion and the incorporation of the ions into the crystal lattice at the growth site.<sup>22</sup>

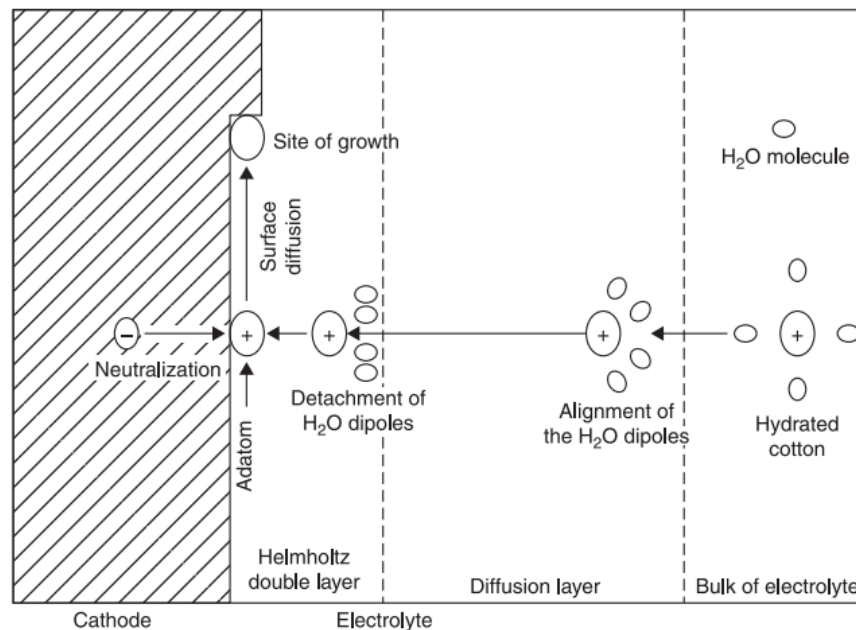


**Figure 4:** Schematic of the steps in cathodic deposition of metals.<sup>22</sup>

#### 1.4 Electrochemical Oscillations

In this thesis, electrochemical oscillations have been observed during the fabrication of CuS nanoparticles. Electrochemical processes in connection with oscillations of current or potential have been known for more than a century.<sup>24,25</sup> Interest involving the spontaneous oscillations of electric current or potential have been recognized as an interesting subject of study and, in the past few decades, the field has expanded greatly as clear-cut experimental examples of concepts in dynamical systems theory have been discovered.<sup>25</sup> The frequent appearances of oscillations and pattern formation in electrochemistry is not surprising due to the electrochemical kinetics being inherently nonlinear.<sup>26</sup> Additionally, electrochemical experiments are usually conducted by imposing external constraints such as the application of a constant potential drop between two electrodes which creates a far from equilibrium situation.<sup>26</sup>

In order for a chemical system to exhibit oscillations, the system must be far from equilibrium. This implies that the system must contain an entropy producing process which is capable of compensating for the decrease of entropy.<sup>27-29</sup> The compensation for the decrease of entropy is necessary due to the second law of thermodynamics which states that any creation of order is accompanied by a decrease in entropy.<sup>28</sup> Due to the formation of dissipative structures which form to account for the decrease in entropy, the oscillations that occur in a system are taking place towards equilibrium.<sup>27-29</sup> From a kinetic perspective, a system must contain the presence of a nonlinear feedback in its kinetics in order to produce nonlinear behavior.<sup>29,30</sup> This implies that the reaction will not evolve in a simple linear fashion.<sup>29</sup> In an autocatalytic reaction, the reaction rate increases

as the concentration of a product increases. This is the result of the formation of a product that catalyzes its own production.<sup>27,29,30</sup> Through feedback loops, the system can maintain nonlinear behavior.

In dynamic systems, a source of instability must be present. In electrochemical systems, instability occurs when the slope of a current / potential graph is negative.<sup>27</sup> The term negative differential resistance (NDR) is utilized to refer to this characteristic.<sup>27</sup>

There are different types of electrochemical oscillators: negative differential resistance oscillators (NDR), potentiostatic oscillators, and capacitance mediated positive differential resistance oscillators (CMPDR).<sup>27,29,31,32</sup> NDR oscillators can be further subdivided to three classes: N-shaped NDR (N-NDR), hidden NDR (HN-NDR), and S-shaped NDR (S-NDR).<sup>27,29,33</sup>

In N-NDR systems, the electrode potential is the autocatalytic variable, or the positive feedback variable.<sup>27</sup> In this type of oscillator, the shape of the I-E dependence (current – electrode potential) resembles the letter N (N-shaped stationary polarized curve).<sup>27</sup> As the oscillations of the N-NDR type can only be seen in the current, it is only observable under potentiostatic conditions.<sup>27,29</sup> Oscillations related to the N-NDR region are considered the results of the positive feedback involving the electrode potential.<sup>27</sup> The electrode potential increases until the slow chemical, negative feedback variable, takes control over the system's dynamics.<sup>27</sup> These oscillations require an ohmic resistance in series with the electrochemical interface.<sup>32</sup>

In HN-NDR electrochemical oscillators, the electrode potential remains the autocatalytic variable. However, the N-NDR region in the stationary current-electrode

potential curve is partly or entirely hidden by another process.<sup>27,32</sup> The negative impedance can remain hidden if at least two processes overlap: a fast one with NDR characteristics and a relatively slow one with the positive slope.<sup>27,32</sup> The slow process manifests itself only at low frequencies in the spectrum, while the faster process that is characterized with the negative impedance reveals itself for intermediate frequencies.<sup>27</sup> Typical impedance spectra of the systems that can exhibit oscillations can be compared with Nyquist spectra.<sup>27</sup> As shown in Figure 5, the NDR region and hidden NDR region can be identified utilizing a Nyquist spectrum.

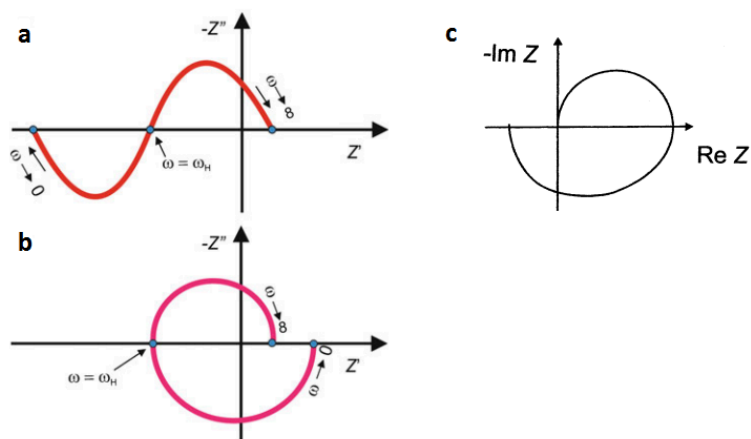


**Figure 5:** Schematic shape of the Nyquist diagrams for the systems: (a) N-NDR region; (b) hidden NDR region; and (c) S-NDR region.<sup>27</sup>

In S-shaped NDR systems, the shape of the I-E dependence resembles the shape of an S as shown in Figure 6. In S-NDR systems, the chemical species becomes an activator, while the electrode potential takes the role of an inhibitor (negative feedback variable).<sup>27</sup> The electrode potential supplies the slow negative feedback.<sup>27</sup>

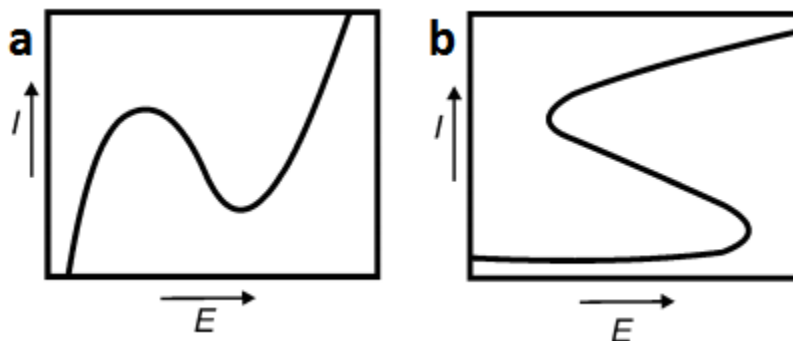


**Figure 6:** Comparison of I-E dependencies for the (a) N-shaped and (b) S-shaped NDR characteristics.<sup>27</sup>

In strictly potentiostatic oscillations, the electrode potential is a parameter and the oscillatory mechanisms involves only the chemical species.<sup>32</sup> There are also other mechanisms which would lead to oscillations, such as convection caused by gas bubbles.<sup>32</sup>

Capacitance mediated positive differential resistance oscillators (CMPDR) exhibit features that are distinct from the systems with an NDR.<sup>32</sup> This type of oscillator is driven by the formation and dissolution of an inhibiting surface layer on the electrode surface.<sup>29,32,34</sup> Additionally, the oscillations occur on a branch of positive differential resistance.<sup>29,32,34</sup> Other features discussed by Zensen *et al* include that oscillations occur around a current plateau in CVs and in relevant parameter regions where there is no hint to the existence of bistability in CVs. Another feature is that no external resistor is required.<sup>29,32</sup>

## **Chapter 2: Project Overview**

### 2.1 Research Objectives

The objectives of the project are to develop a novel electrochemical approach to prepare copper sulfide nanoparticles, to determine quantitative parameters for the as-prepared compounds as an electrochemical sensor, and to gain insight into the sensor's electrochemical behavior based on its morphology. In this study, a series of experiments have been performed in order to optimize the fabrication process which include varying the length of the electrode, reaction time, potential applied during fabrication, and concentration of sodium bisulfite. Scanning electron microscopy was utilized to analyze and relate the morphologies of different conditions to their detection capabilities.

### 2.2 Experimental Methods

Glassy carbon electrodes (GCE) were purchased from CHI Instruments. The bare GCE was first polished with 0.3 $\mu$ M and 0.05 $\mu$ M alumina powder on emery paper. The GCE was ultrasonically cleaned in acetone followed by water for 2-3 minutes each, and rinsed with double distilled water (ddH<sub>2</sub>O). The GCE is used as the working electrode to undergo potentiostatic reactions in electrolytic solution of varying concentrations of sodium bisulfite at various potentials. The supporting electrolyte is 0.1M sulfuric acid. Various reaction times ranging from 10 to 60 minutes were studied in order to determine the best time interval for fabrication. The reference electrode used was Ag/AgCl, while the counter was a copper wire. A four-electrode system was also developed in this

research in which a potentiostat was attached to the counter and a second Ag/AgCl reference while the standard three-electrode setup was attached to the VoltaLab PGZ 100 electrochemical station as shown in Figure 7.

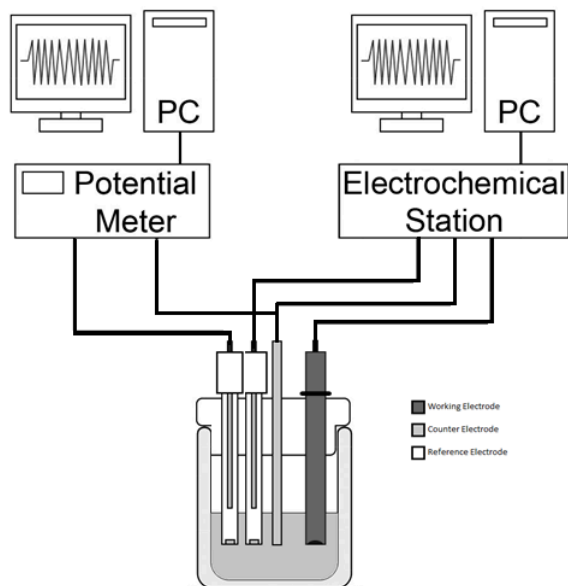


**Figure 7:** Four electrode system for fabrication of the modified electrode via potentiostatic reaction.

After undergoing a period of potentiostatic reaction, all electrodes were rinsed with double distilled water. The copper wire which was the counter electrode during the synthesis of CuS nanoparticles was investigated as an electrochemical sensor. The analyte focused in this thesis is glucose. For the detection of glucose, the CuS coated electrode undergoes 10 cycles of cyclic voltammetry (CV) between -200mV and 800mV at a rate of 100mV/sec. in 0.1M NaOH with varying glucose concentrations ranging from 0.5mM to 2mM. An Ag/AgCl reference and a platinum wire counter electrode were used for all glucose detection experiments. The above processes took place under room temperature of  $23 \pm 1^\circ\text{C}$ .

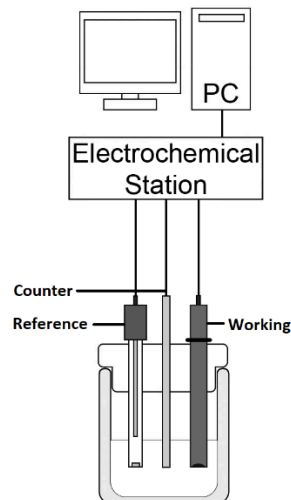


**Figure 8:** Three electrode system for the detection via cyclic voltammetry (the same as Figure 1).

Sodium hydroxide was purchased from EM Science. Sulfuric acid (95-98%) was obtained from ACP Chemicals Inc. Sodium bisulfite was obtained from Aldrich. D-(+)-glucose was obtained from Oakwood Chemical. Ammonium hydroxide was obtained from Fisher Scientific. All reagents were used as received. Scanning electron microscopy (SEM) images were taken on a FEI Quanta 200 FEG microscope.

## Chapter 3: Results and Discussion

### 3.1 Fabrication of the Copper Sulfide Sensor on the Counter Electrode

In order to fabricate the modified copper sulfide based electrochemical sensor on to the copper counter electrode, an electrochemical technique called chronoamperometry is utilized. This technique is time dependent and applies a constant potential to the working electrode. A constant potential of 1500mV was applied to the GCE working electrode. The Ag/AgCl reference was utilized and the reaction was completed in an electrolytic solution of 0.3M sodium bisulfite and 0.1M sulfuric acid. The copper wire that was utilized as the counter electrode was set to a length of 1.0cm.

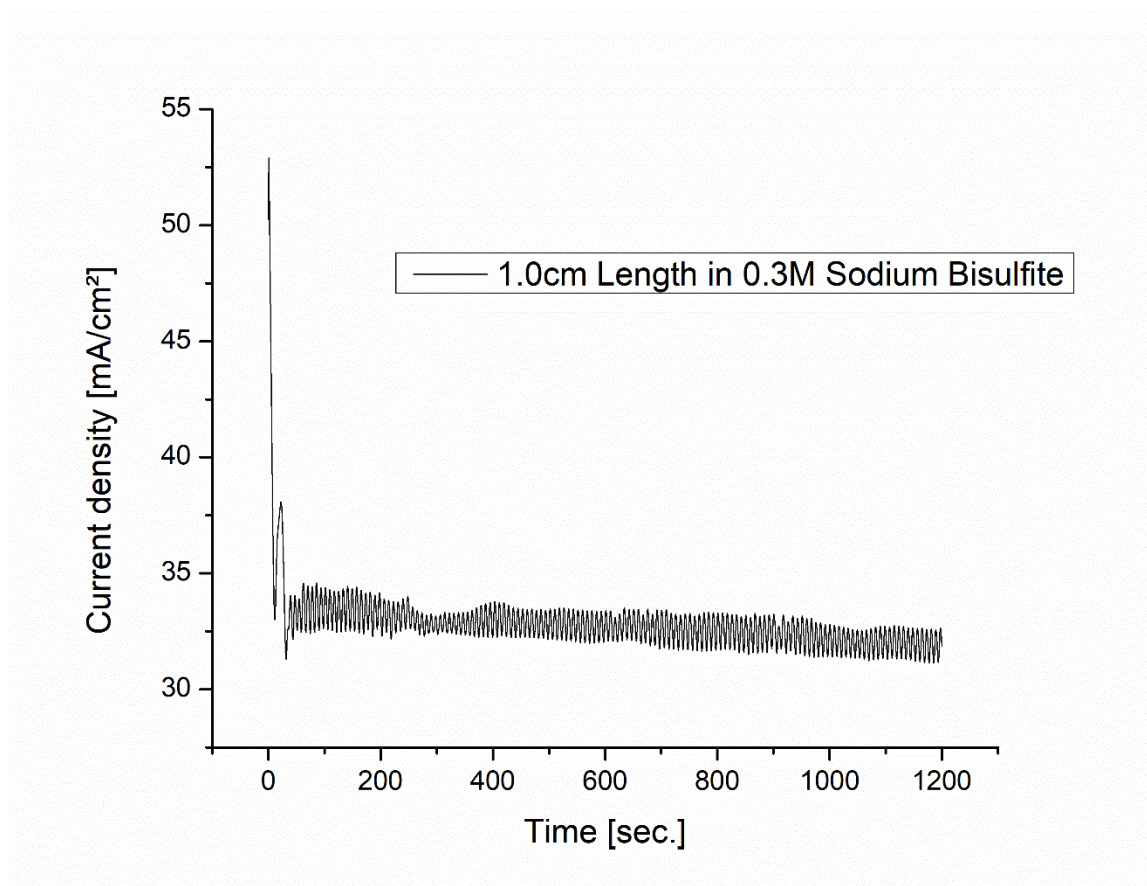


**Figure 9:** Potentiostatic time series of the fabrication of a modified copper wire electrode.

As shown in Figure 9, the current vs time graph created from potentiostatic experiments features the oscillatory behavior during the fabrication of the modified copper electrode. Please note that the above graph demonstrates the activity occurring on the GCE working electrode. It can be seen that an oscillatory pattern occurs at around 40 seconds into the reaction. The current density drop observed in the plot is attributed to the concentration decrease of sulfite at the electrode/electrolyte interface. Initially, prior to the application of the external potential, the concentration across the media is homogenous, where no concentration gradient is present. Following the application of a large positive potential, the oxidation of active electrolyte leads to the development of a concentration gradient. The larger the potential applied, the larger the drop observed as a result of the concentration gradient being larger, until the highest concentration gradient is reached.

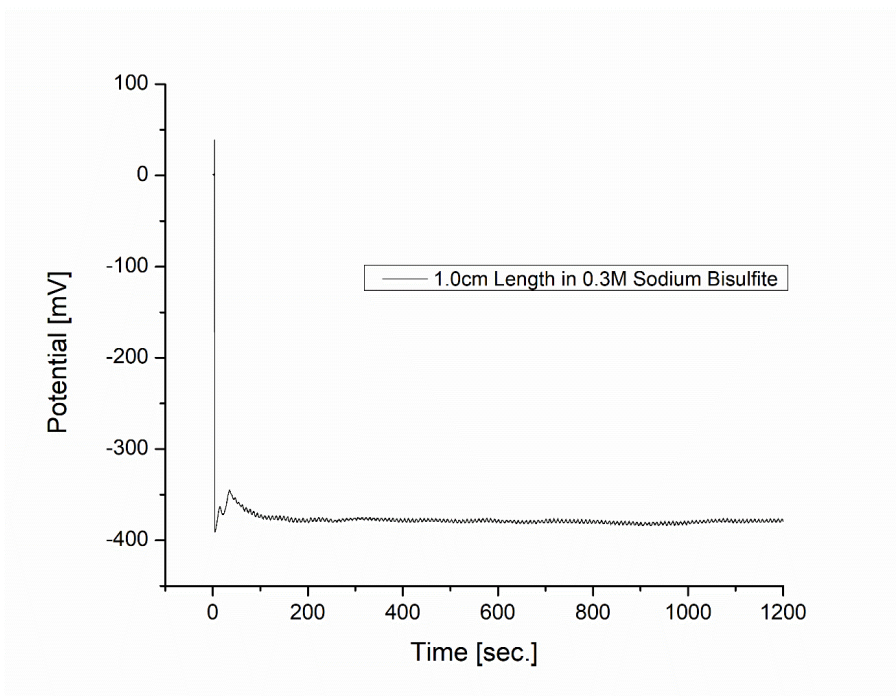


**Figure 10:** Time series of the potential of the counter electrode recorded during the fabrication of a CuS nanoparticles.

Figure 10 shows the potential of the copper counter electrode recorded during the potentiostatic reaction presented in Figure 9. Oscillatory behavior similar to that observed at the GCE working electrode can be seen here. Further discussions on this similarity will be presented in the next chapter. During the fabrication process, a dark deposit forms on the copper counter electrode and coats the entire 1.0cm length. This dramatic color change is evidence that the electrodeposition was successful and the modification of the counter electrode had occurred.

Following the fabrication of the modified counter copper sulfide electrodes, the performance of these modified electrodes as an electrochemical sensor has been examined through cyclic voltammetry in glucose solution. These experiments also serve as a guidance for the optimization of the amount of time required for the fabrication of the modified electrode. In these cyclic voltammetric experiments, each modified copper wire was set to a length of 1.0cm and was utilized as the working electrode. Each CV was conducted within a potential range of -200mV to 800mV in a solution containing 0.5mM glucose and 0.1M sodium hydroxide. A scan rate of 100mV/sec was utilized with a counter Pt electrode and an Ag/AgCl reference.

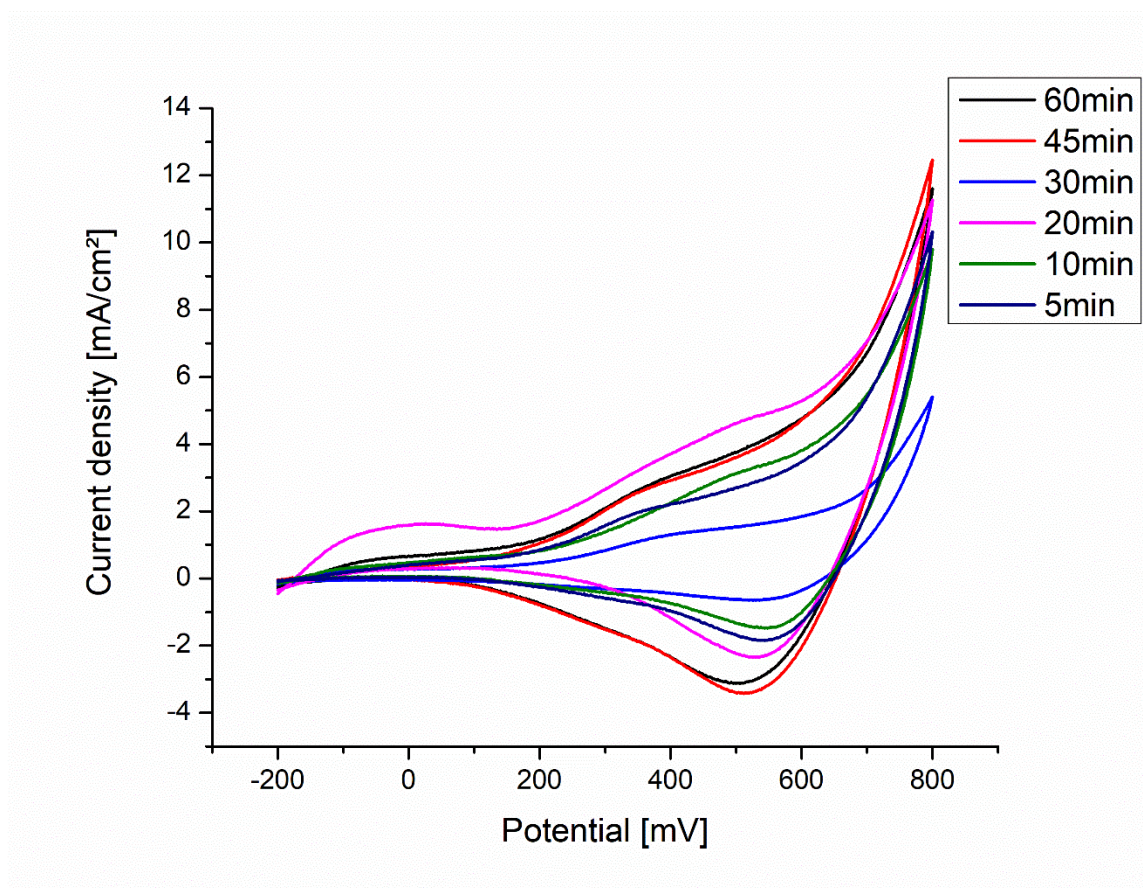


**Figure 11:** A series of CVs that compare the various modified copper wires with varying times of fabrication.

As shown in Figure 11, the modified copper wire electrode with a 20 minute (1200 seconds) fabrication time interval exhibits the largest oxidation glucose peak at around 450mV compared to the ones fabricated at other time intervals. The oxidation peak observed in Figure 11 during the forward scan matches the anodic glucose peak observed in literature.<sup>35,36</sup> The peak at around 0mV for the 1200 second modified copper wire is likely due to the oxidation of the copper.<sup>35</sup> The electrode prepared with a fabrication time of 5 minutes (300 seconds) seemed to exhibit the worst detection capabilities. Thus, a 1200 seconds fabrication time interval has been the focus of the following investigations.

### 3.1.1 Analysis of Oscillatory Behavior

An investigation into the possible correlations between the working electrode and counter electrode was completed. The oscillatory behaviors are caused by the instabilities introduced into the system due to the positive current which maintains reaction conditions away from equilibrium.<sup>25</sup> The current results in the net oxidation and reduction reactions at the GCE working electrode and copper counter electrode, respectively.

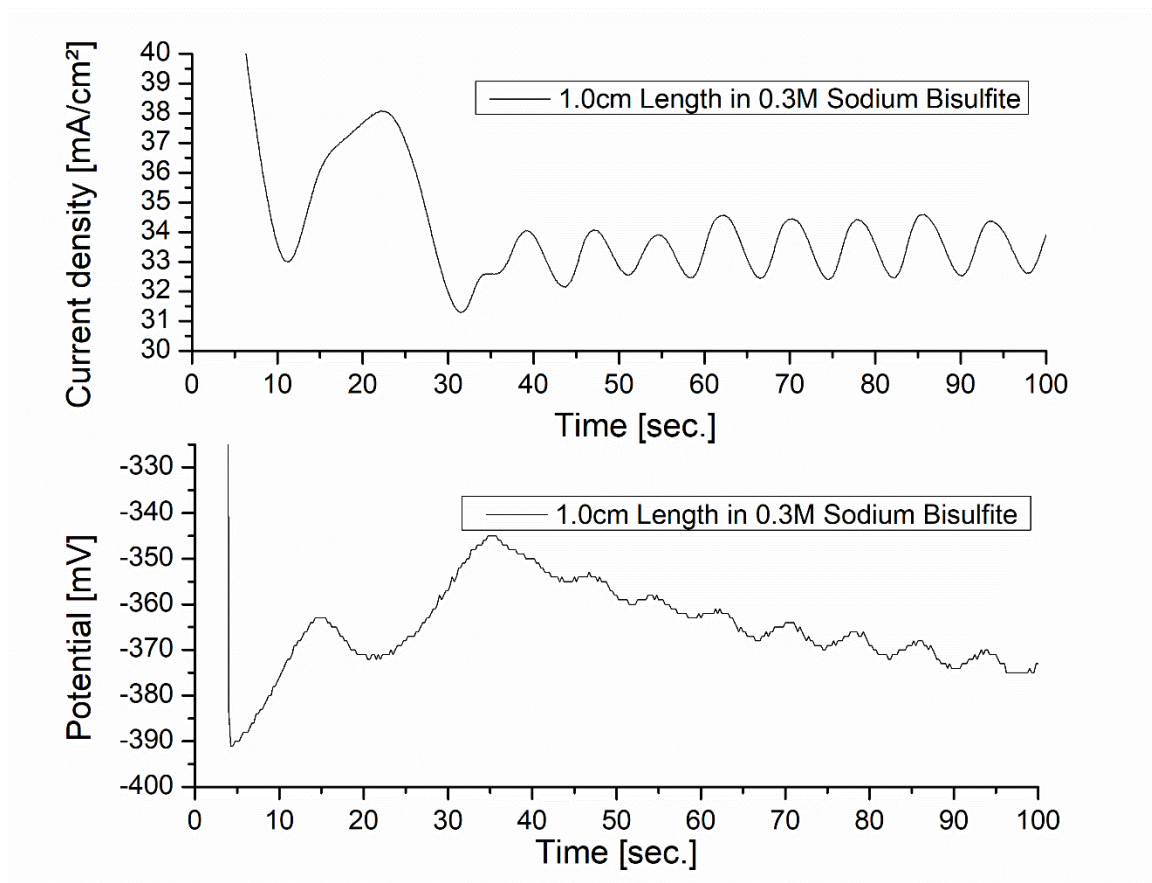


**Figure 12:** Comparison of the potentiostatic time series at the GCE and the time series of the potential value at the counter for the time interval of 0 to 100 seconds.

In Figure 12, the oscillatory pattern for the GCE working and the copper counter electrode is compared which demonstrates the detailed close view of the initial behavior observed from 0 to 100 seconds. It can be observed that the behavior from 0 to 30

seconds seems inversely related. This matches expectations as during the potential drop, oxidation at the working GCE occurs. The corresponding net reduction occurs at the counter electrode. As a positive potential is applied, at the GCE working electrode, oxidation occurs which moves the system out of equilibrium.

$$E = E^o - \frac{RT}{nF} \ln \ln \left( \frac{[red]}{[ox]} \right) \quad [1]$$

The Nernst equation shown in equation [1] can be utilized to determine the dominating redox species based on the data obtained from the time series of the potential at the counter electrode recorded during the fabrication of CuS nanoparticles. In the Nernst equation, the cell potential at the temperature of interest is  $E$ , whereas  $E^o$  is the standard cell potential,  $R$  is the universal gas constant,  $8.314 \text{ J K}^{-1} \text{ mol}^{-1}$ ,  $T$  is the temperature in kelvins,  $F$  is Faraday's constant,  $9.648 \times 10^4 \text{ C mol}^{-1}$ , and  $n$  is the number of electrons transferred in the cell reaction or half-reaction. The  $[ox]$  and  $[red]$  correspond to the activities of the oxidized and reduced species, respectively.

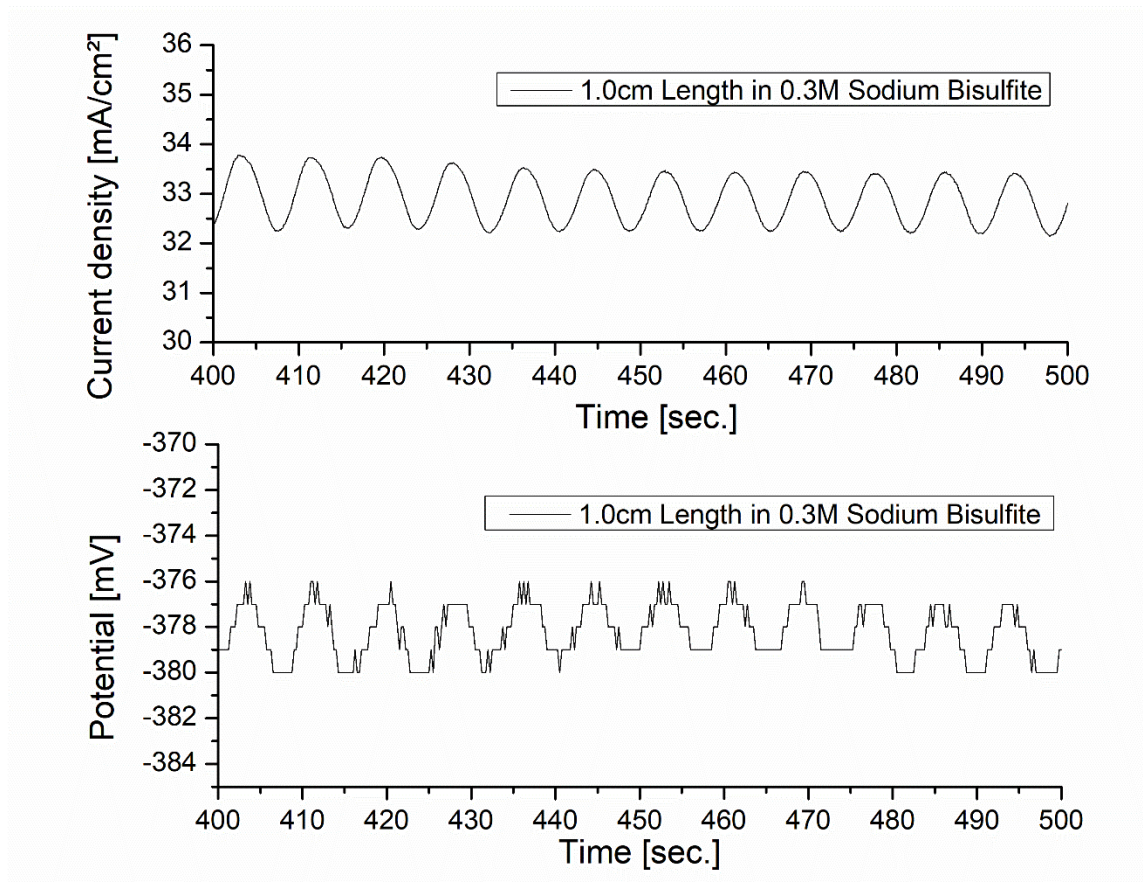


**Figure 13:** Comparison of the potentiostatic time series at the GCE and the time series of the potential value at the counter for the time interval of 400 to 500 seconds.

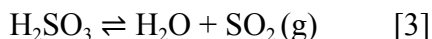
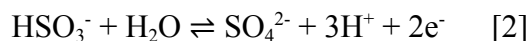
As per Figure 13, a comparison of the oscillatory behavior is analyzed at the time interval of 400 seconds to 500 seconds. Strikingly similar results are observed between the time series recorded at the GCE working and the copper counter electrode. The oscillatory pattern observed and frequency of the amplitudes closely align when comparing the time series of the GCE working and copper counter electrode. The overall net potential observed from the time series of the potential at the counter electrode provides insight on the specific electrochemical species. From the potentiostat time series

shown in Figure 13, a cell potential (E) of -378mV can be utilized in the Nernst Equation [1].

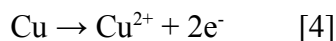
According to literature,  $S(s) + 2e^- \rightleftharpoons S^{2-}$  has a standard cell potential of -407mV.<sup>37</sup> The standard reduction cell potential found in literature and the experimental cell potential of -378mV closely favors the reduction of S(s) to S<sup>2-</sup>. Thus, the dominating species at the counter electrode can be predicted with high confidence to be S<sup>2-</sup>.

### 3.1.2 Proposed Mechanism of the Formation of Copper Sulfide

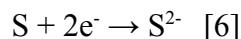
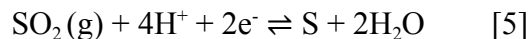
Copper sulfide forms by the oxidation of copper metal in the presence of sulfur, whereas in the presence of water, a continuous solid-state reaction occurs without passivation by the product. The copper counter electrode is utilized to close the current circuit during potentiostatic experiments while a glassy carbon electrode is utilized as the working electrode. At the GCE working electrode (anode), oxidation of sodium bisulfite occurs in acidic conditions as shown in reaction [2]:



The solution contains sulfuric acid which causes reaction [3] to undergo. At the counter electrode (cathode), net reduction occurs. As shown in reaction [4], oxidation of copper is predicted to occur in which the Cu wire loses two electron resulting in  $\text{Cu}^{2+}$ .



Besides the oxidation of copper, sulfur dioxide is further reduced to  $\text{S}^{2-}$  as shown in reaction [5] and reaction [6].



The copper counter electrode is then surrounded by the product of the sulfur dioxide reduction which catalyzes the reaction to form the  $\text{Cu(II)S}$  deposit. The reduction of sulfur dioxide accounts for the net reduction behavior observed. This discovery is

interesting as it is a case in which the cathode counter electrode is both oxidized and reduced. It also is a case in which the counter electrode participates in the reaction.

### 3.2 Imaging the Electrode Surface

A series of SEM imaging was completed for various conditions in order to compare the morphology and relate it to its detection properties. Figures 14 show SEM samples created at 0.3M sodium bisulfite concentrations. A leaf-like structure can be observed at a length of 1.5cm in Figure 14 (a). At a length of 0.5cm in Figure 14 (b), rows of strips can be analyzed. It is predicted that the formation of the leaf like structures contribute to better sensitivity to glucose. Figures 15 were SEM samples fabricated with potentiostatic experiments at high concentration (0.5M sodium bisulfite) with various lengths. As shown in Figure 15 (a), a length of 1.5cm shows the formation of granule-like structures. As the length used during the fabrication was decreased, the morphology changed correspondingly. In the 1.0cm (b) and 0.5cm (c) SEM images of Figure 15, it is noticeable that the granules observed become smaller in size. It is reflected in the next section that a length of 1.0cm has better detection of glucose than a length of 0.5cm. Energy-dispersive X-ray spectroscopy (EDS) was also done which demonstrated that the sample contained copper and sulfur confirming the presence of copper sulfide as shown in Figure 16. Further SEM imaging can be done to relate other conditions to their detection properties.

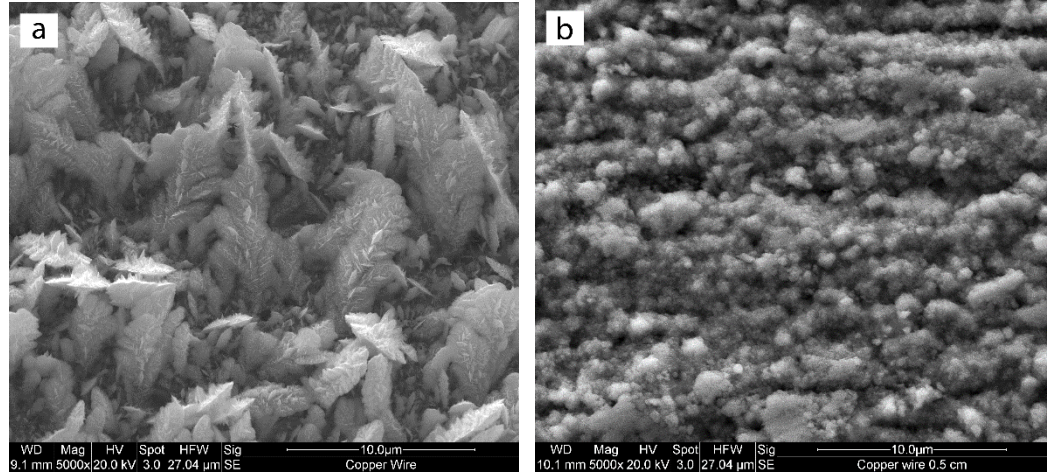


**Figure 14:** SEM Images at 5000x magnification showing the morphology of the modified copper counter electrode for (a) 1.5cm length and (b) 0.5cm length in 0.3M sodium bisulfite concentration.

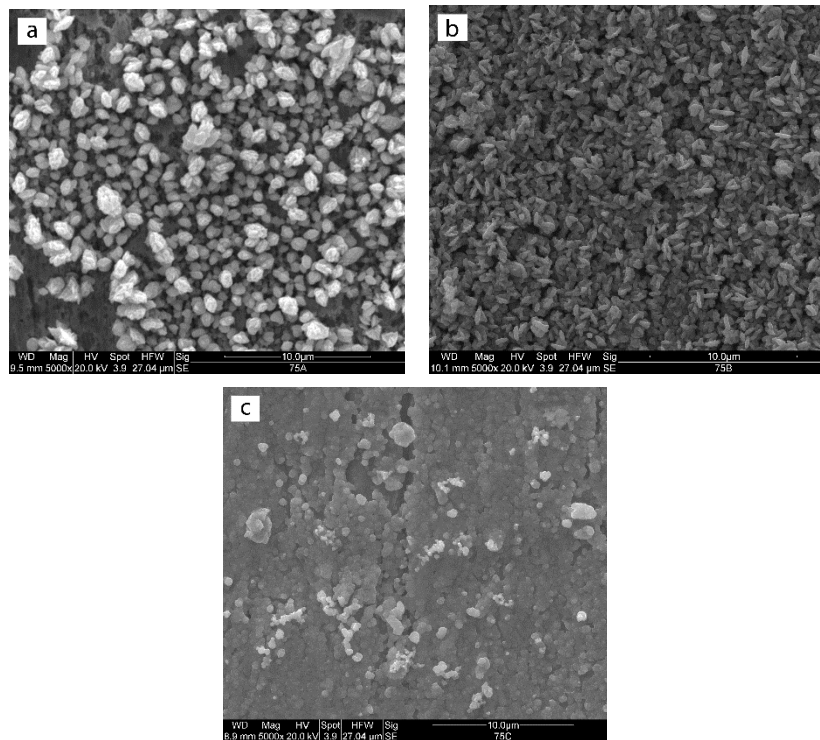
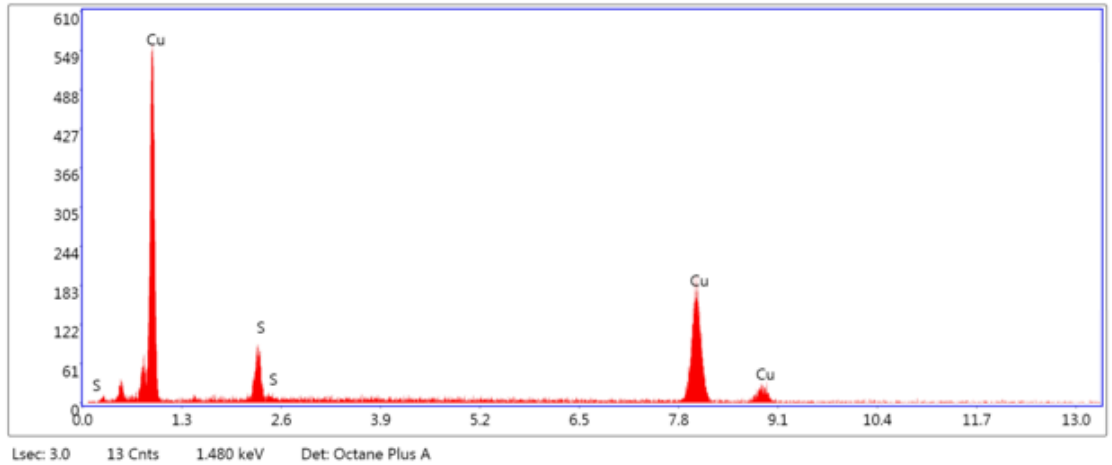


**Figure 15:** SEM Images for the modified counter copper sulfide electrode at 5000x magnification for (a) 1.5cm, (b) 1.0cm, and (c) 0.5cm length in 0.5M sodium bisulfite concentration.



**eZAF Smart Quant Results**

Element	Weight %	Atomic %	Net Int.	Error %	Kratio	Z	A	F
S K	8.88	16.19	508.44	12.18	0.0630	1.1657	0.6054	1.0047
CuK	91.12	83.81	1781.75	3.67	0.8947	0.9820	0.9986	1.0014

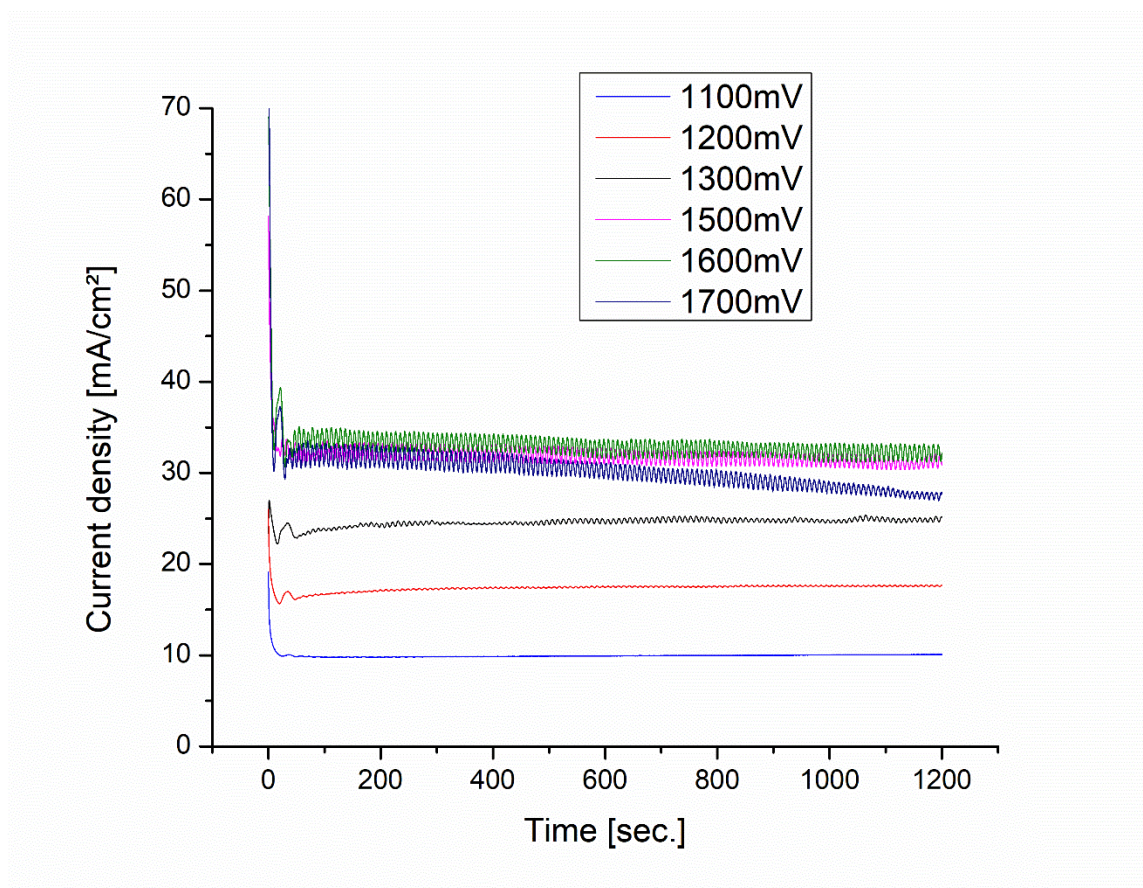
**Figure 16:** EDS of the SEM sample shown in Figure 15 (a).

### 3.3 Fabrication Optimization

A variety of optimizations in regards to the CuS fabrication have been pursued on the basis of their responses to the electrochemical oxidation of glucose. More specifically, series of experiments adjusting the parameters: potential, sodium bisulfite concentration, and length of the copper wire were investigated in this study.

#### 3.3.1 Investigating the Effects of the Applied Potential

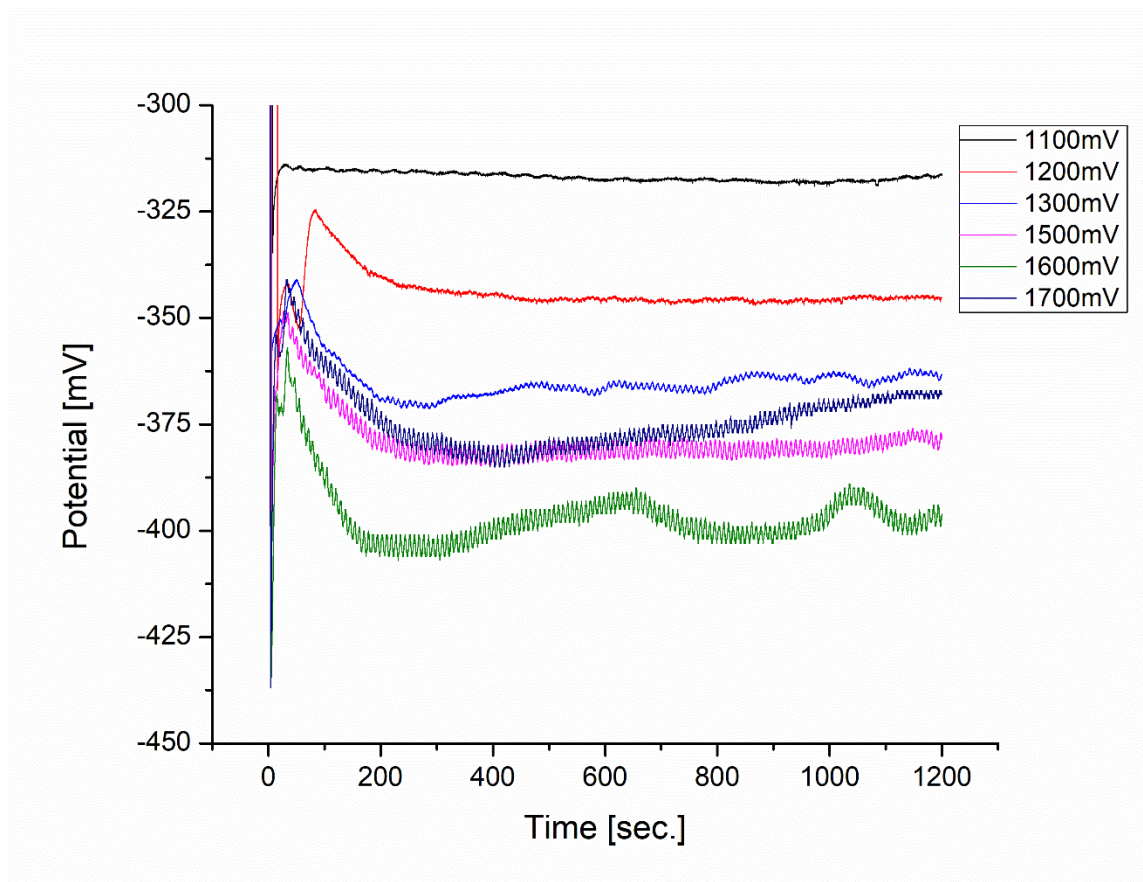
During the investigation of the CuS fabrication process, a series of different potentials from 1100mV to 1700mV were explored. Each experiment was conducted in a solution containing 0.3M sodium bisulfite and 0.1M sulfuric acid for the duration of 1200 seconds. As shown in Figure 17, at lower potentials applied to the working GCE electrode, the current density is noticeably lower. At the applied constant potential of 1100mV, oscillations with very small amplitude can be observed at the current density of *ca.* 10mA/cm<sup>2</sup>. An increasing trend in which the higher the potential applied, the higher the amplitude and current density is observed. The lower current density, which is the amount of electric current flowing per unit cross-sectional area of a material, reflects that less oxidation activity is occurring. As the applied potential increases, the underlying oxidation activity at GCE is expected to increase, leading to the increase of the average anodic current density.



**Figure 17:** Potentiostatic time series at the working electrode during the fabrication of the CuS nanoparticles at various potentials.

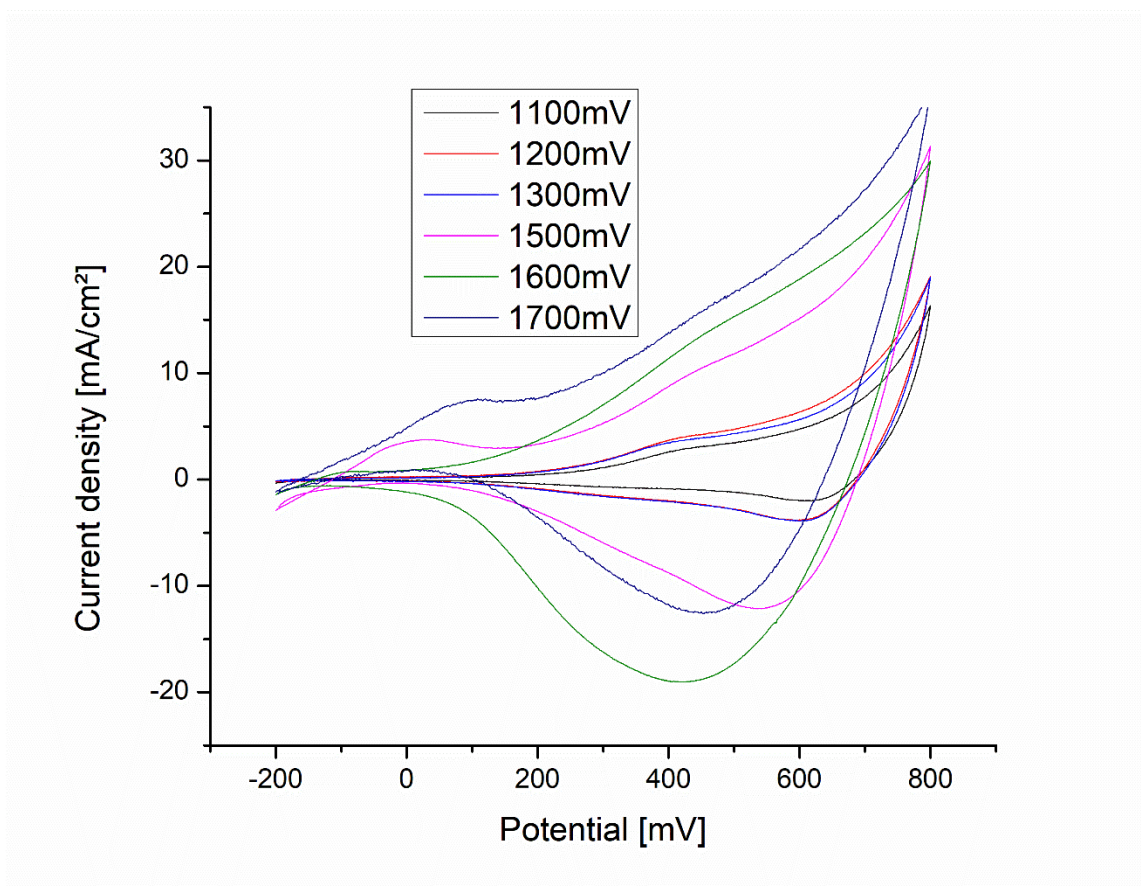
Figure 18 shows the time series of the potential of the counter electrode, which reflects the activity occurring at the copper counter electrode during the above potentiostatic fabrication process. At lower applied potential, smaller oscillations are observed similar to the trend seen on the working electrode. Additionally, as the applied potential increases, the amplitudes of the oscillations also increase. This behavior can be understood based on the fact that the counter electrode serves as a follower to meet the activity taking place at the working electrode, i.e., the oxidation of bisulfite in this research. As the applied potential increases, which leads to stronger current at the working electrode, the potential recorded at the counter electrode becomes more negative, signaling stronger reduction activity. Phenomenologically, the layer of copper

sulfide deposit becomes thicker when a higher potential is applied. This is because the larger the difference between the excess and the deficit of electrons, the faster the electrons will flow and the greater the current will be. There is an excess of electrons on the GCE anode, and a deficit of electrons on the copper cathode. This results in a higher rate of reaction, thus, causing the copper counter electrode to have a thicker layer of coating at high potential than at low potential. This is consistent with the current density observed in the potentiostatic time series of the GCE working electrode. At low potential, the rate of reaction is slower as shown by the smaller amplitudes of the oxidation-reduction peaks which contribute to less copper sulfide deposit on the counter.



**Figure 18:** Time series of the potential of the counter electrode recorded during the fabrication of a CuS nanoparticles at various potentials.

To compare the fabricated counter electrodes' detection properties, cyclic voltammetry was used in which the modified copper electrodes were used as the working electrodes. It was conducted in 0.5mM glucose and 0.1M sodium hydroxide.



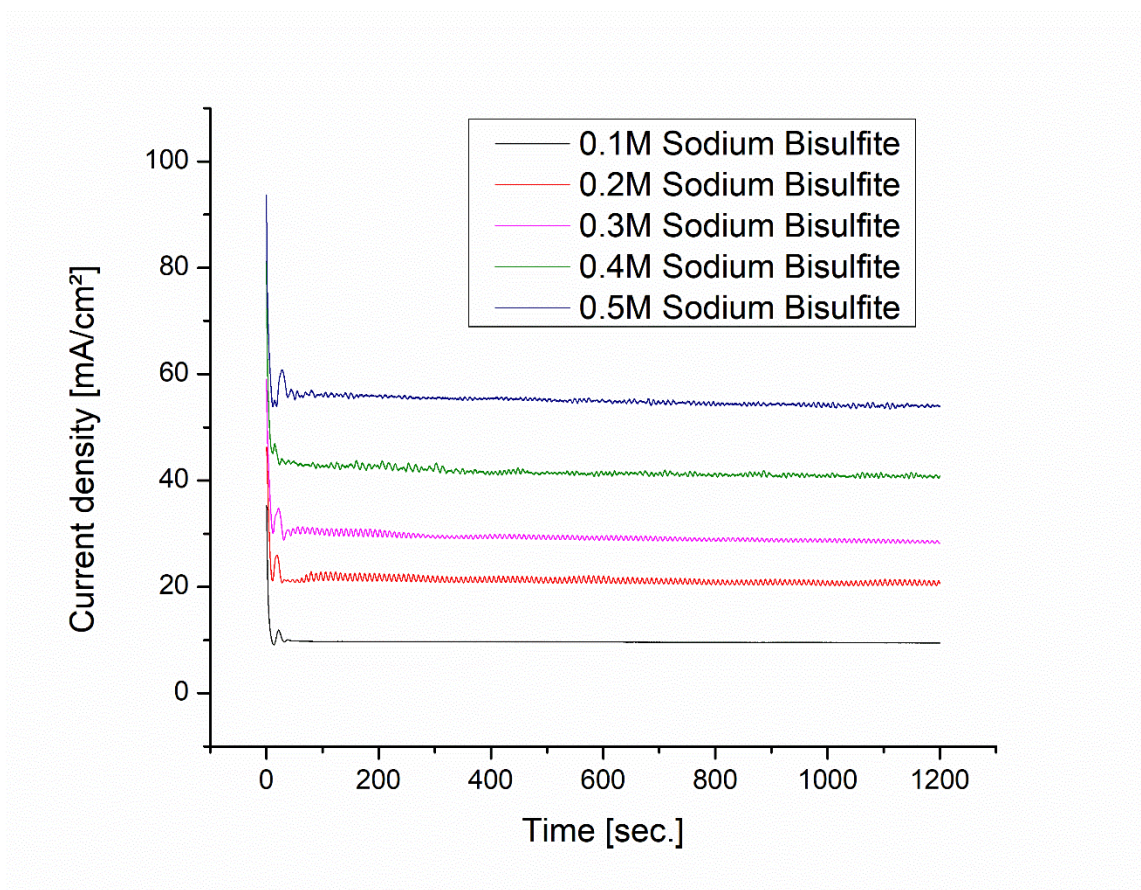
**Figure 19:** CVs of the modified copper electrodes that were prepared with different applied potentials.

Figure 19 demonstrates that the copper electrode that was prepared at an applied potential of 1700mV during the potentiostatic fabrication process has the strongest response to the electrochemical oxidation of glucose based on its current density. Specifically, the anodic glucose peak at *ca.* 450mV is larger and more defined when compared to the modified copper sulfide electrodes fabricated at applied potentials of 1500mV and 1600mV. This indicates that the copper sulfide has a positive influence on

the detection of glucose and that a higher potential increases the sensitivity to glucose. Further experimentation would be required to determine the maximum potential which would be most optimal for the detection of glucose.

### 3.3.2 Optimizing Sodium Bisulfite Concentration

The parameter, sodium bisulfite concentration, was varied in order to determine the ideal concentration that forms CuS nanoparticles which show the best glucose detection capability. Experiments were conducted at constant applied potential of 1500mV for 1200 seconds with the counter electrode length of 1.0cm.



**Figure 20:** Potentiostatic time series of the fabrication of the modified counter electrode with varying sodium bisulfite concentration in 0.1M sulfuric acid solution.

As shown in Figure 20 which reflects the anodic activity at the GCE working electrode, no oscillations could be observed at a concentration of 0.1M sodium bisulfite. Increasing bisulfite concentration results in more defined oscillations up to a concentration of 0.3M. Using a concentration higher than 0.3M would result in smaller,

irregular oscillatory patterns to be observed. The current density is observed to exhibit the trend of being proportional to the increases of concentration, which is expected as reported by literature.<sup>38</sup> At concentrations of 0.5M sodium bisulfite, the current density is around 60mA/cm<sup>2</sup>, whereas the current density is at around 10mA/cm<sup>2</sup> at a concentration of 0.1M sodium bisulfite.

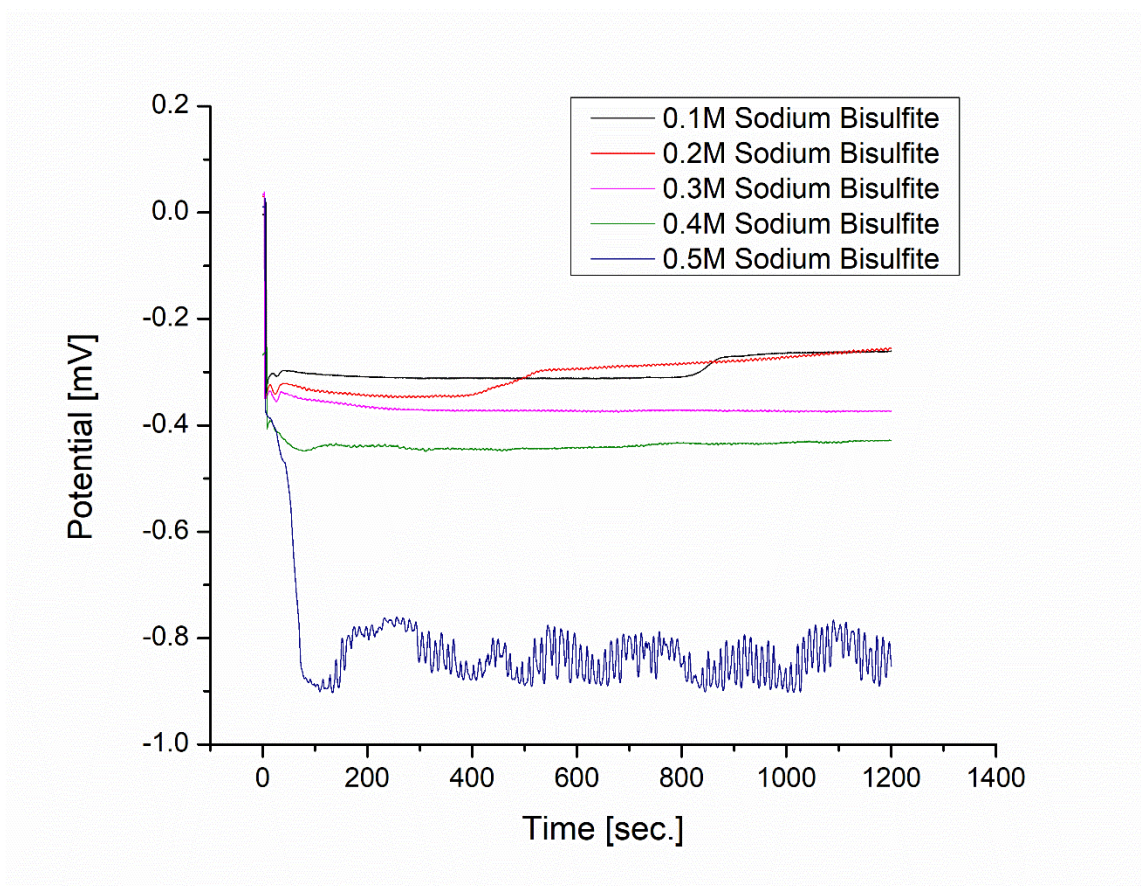


**Figure 21:** Time series of the counter electrode potential during the fabrication of the modified counter electrode with varying sodium bisulfite concentration.

Figure 21 shows the time series of the potential value obtained during the potentiostatic fabrication process. It clearly demonstrates that at 0.3M concentration, the stability of the oscillatory behavior seems to be optimal. At low concentrations such as 0.1M, no oscillatory behavior is observed. At high concentration, it is observed that a

material falls off the counter electrode into solution. It is predicted to be sulfur that is unable to interact with the counter electrode due to the formation of bubbles which will be discussed in the following chapters.

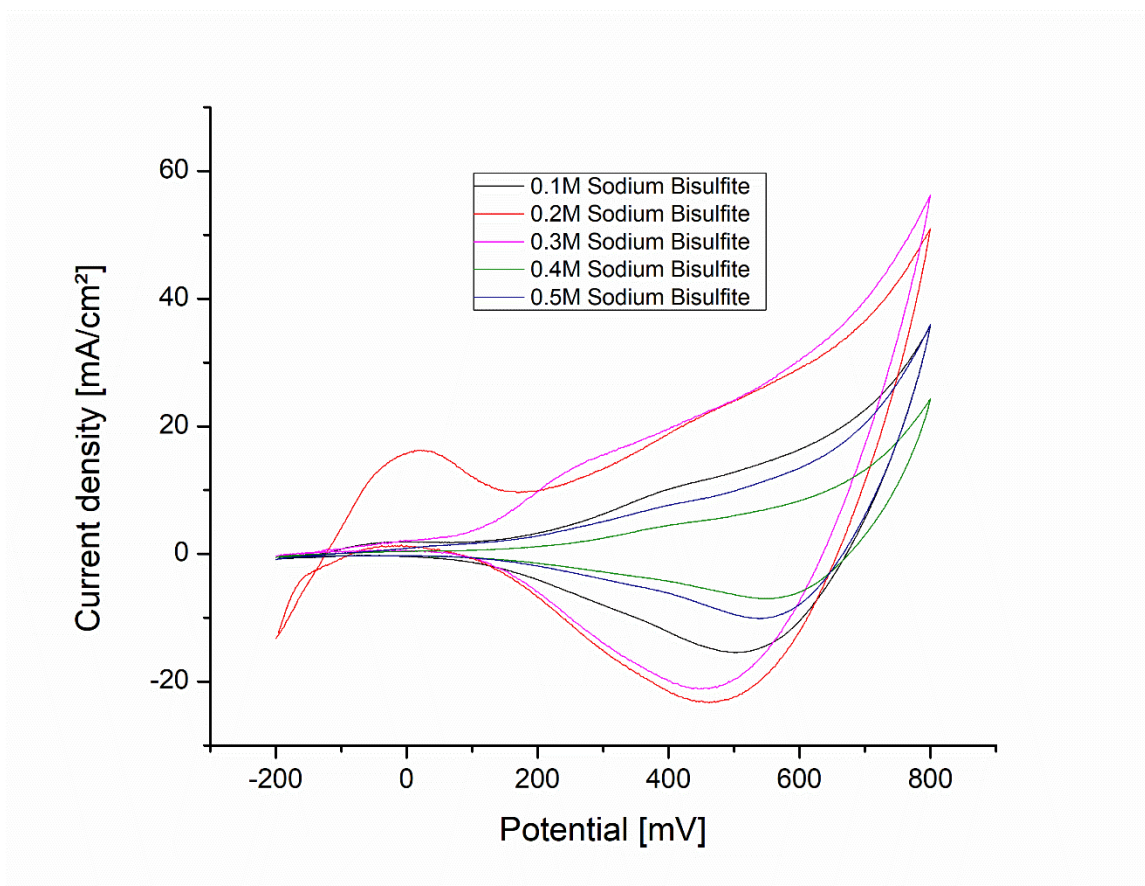


**Figure 22:** CVs of the 10th scan of the modified counter electrodes that were fabricated in varying concentrations of sodium bisulfite during potentiostatic experiments.

CVs presented in Figure 22 illustrate that the modified copper electrodes that were prepared at a moderate concentration of bisulfite has the strongest activity toward the electrochemical oxidation of glucose. A concentration of 0.3M sodium bisulfite appears to be the optimal one, followed by a concentration of 0.2M. The anodic glucose peak at 400 mV is significantly larger and noticeable at 0.3M sodium bisulfite

concentrations. Modified electrodes fabricated at higher concentrations demonstrated detection properties that were sub-par.

### 3.3.3 Optimizing the Length of the Counter Electrode

In addition to the optimization of the applied potential and bisulfite concentration, the lengths of the copper wires also plays a critical role in the formation of CuS deposit because it determines the current density at the counter electrode. Trials in which the length of copper wire (i.e., surface area) was varied was conducted in 0.5M sodium bisulfite. As shown in Figure 23 which is the activity observed at the GCE working electrode during potentiostatic experiments, a smaller length in high concentration of sodium bisulfite results in a more negative potential. Figure 24 shows the activity observed at the counter electrode during the potentiostatic experiments in which smaller length contributes to a more negative potential observed. A variety of oscillatory patterns could be observed which contribute to its difference in morphology at the counter electrode surface. As per Figure 25, it can be observed from the CV that the largest length of 2.0cm in high concentration (0.5M sodium bisulfite) exhibited the best detection. The current density observed at the time of fabrication contributes to the detection and relates significantly to the surface area. At low concentrations (0.1M sodium bisulfite) with a short length of 1.0cm, detection has better performance than at high concentrations (0.5M sodium bisulfite) according to Figure 22 shown previously. This would validate a trend that at high concentration of sodium bisulfite and small surface area length, fabrication is less favorable than with large surface area. This is because as the concentration of sodium bisulfite increases, the surface area of the counter electrode in which the circuit closes requires to be even larger in order to be able to accommodate the large difference in current density. The length of 1.0cm during the trials of Figure 21 utilized in 0.5M

sodium bisulfite concentration is not large enough to accommodate the large difference in surface area, thus, deposition of the copper sulfide was not ideal.

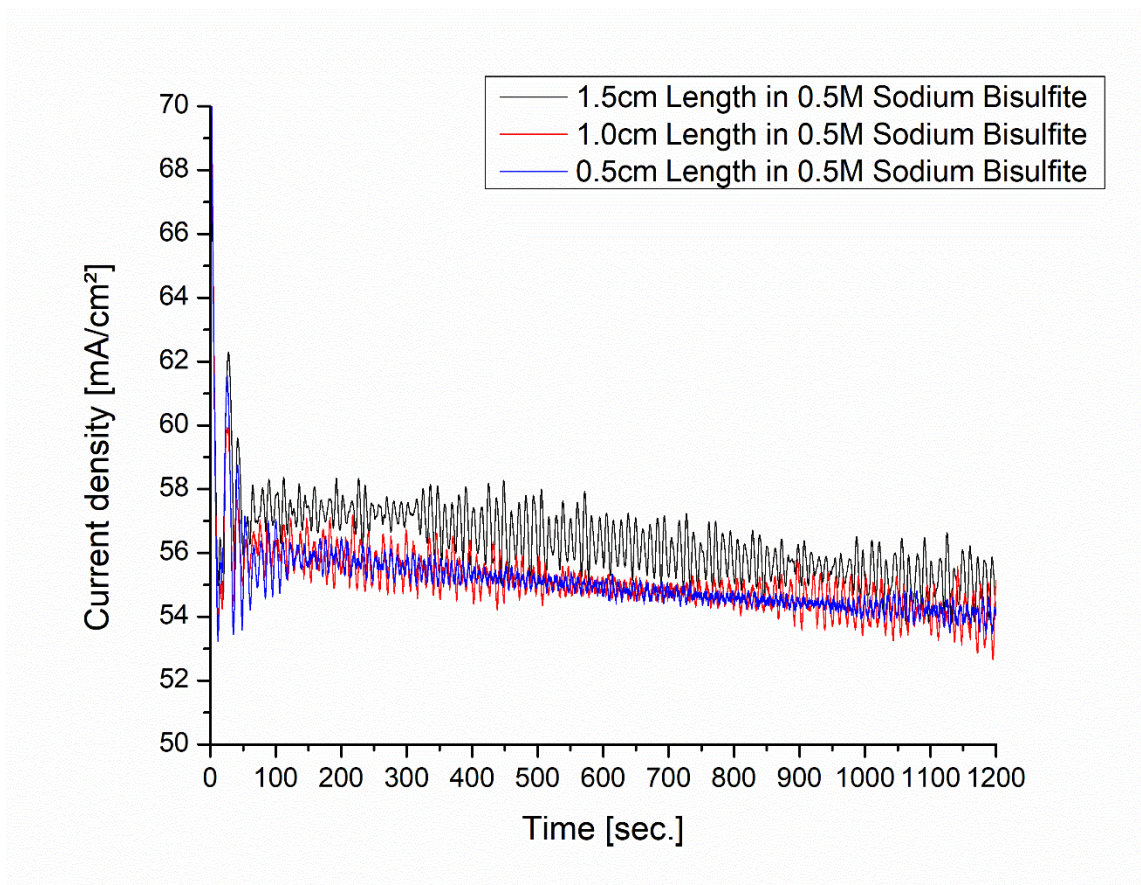


**Figure 23:** Potentiostatic time series of the fabrication of the modified counter electrode in 0.5M sodium bisulfite concentration at varying lengths.

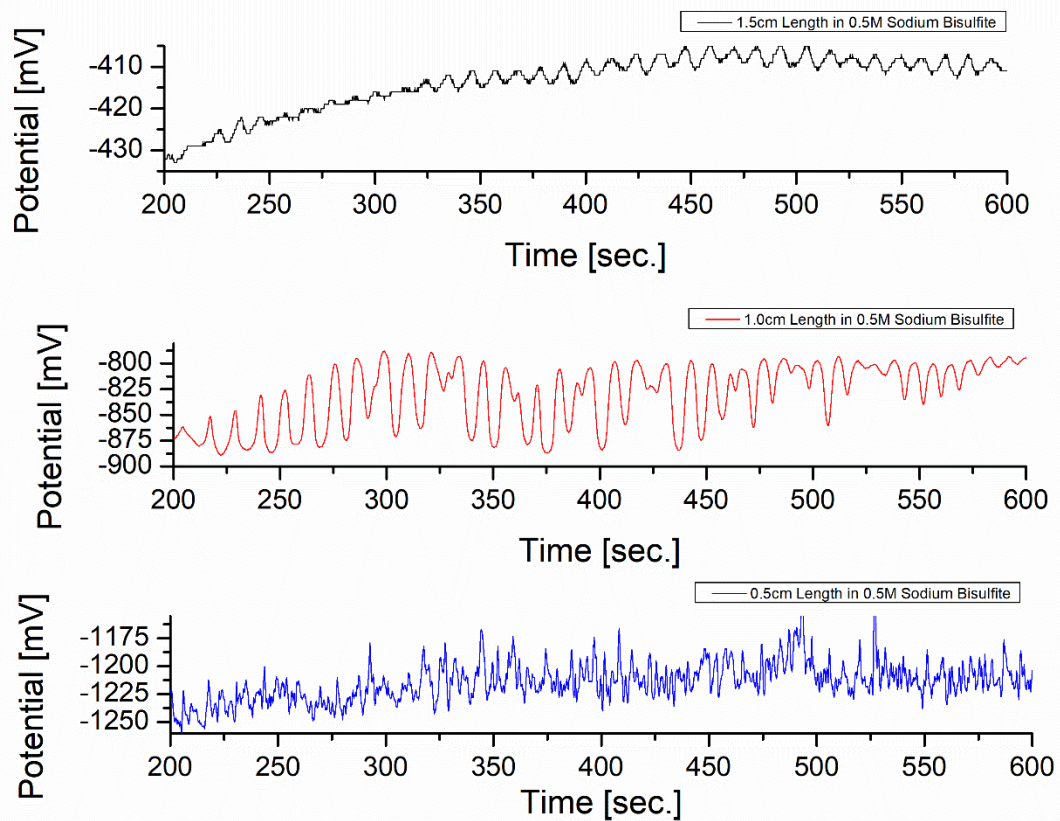


**Figure 24:** Time series of the potential of the counter electrode recorded during the fabrication of CuS nanoparticles for various lengths in 0.5M bisulfite concentration.

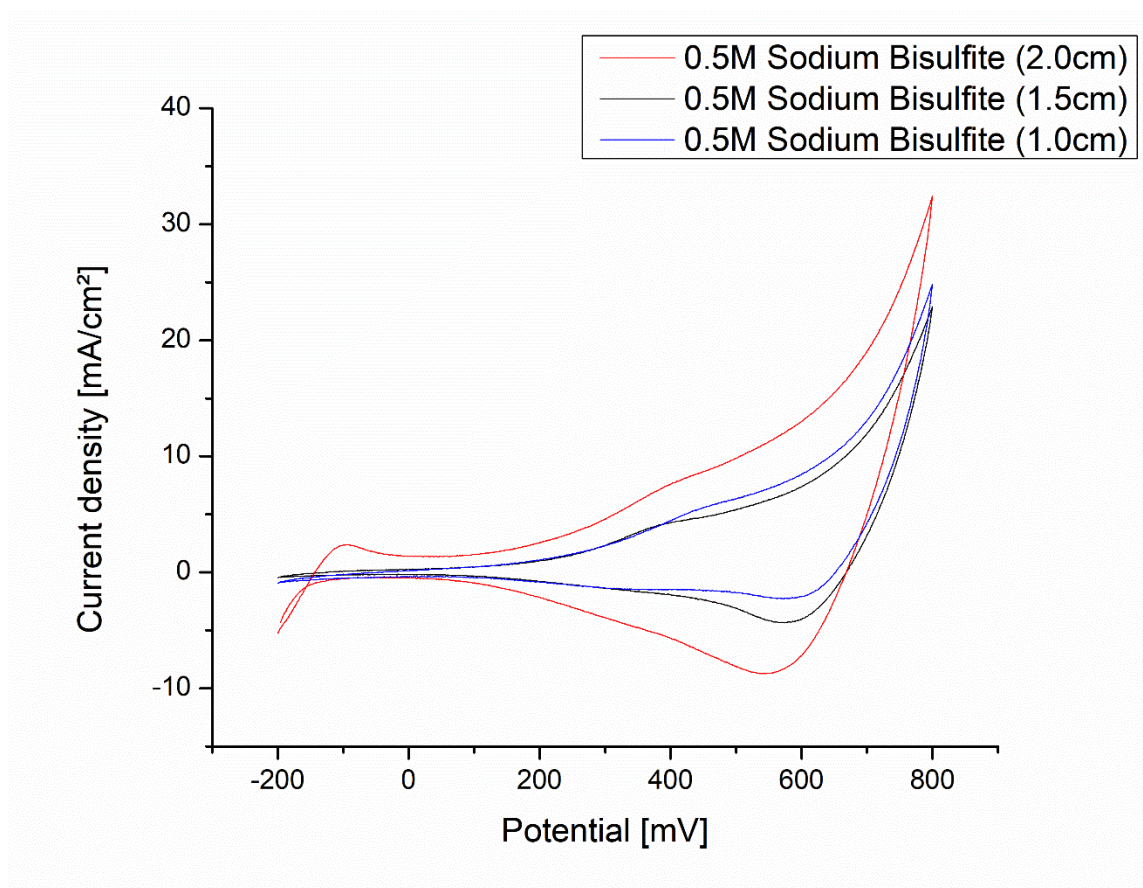


**Figure 25:** CVs of the 10th scan of the modified counter electrodes that were fabricated at various lengths during potentiostatic experiments. Each modified electrode was restricted a length of 0.5cm prior to detection with cyclic voltammetry.

As shown in Figure 26, potentiostatic experiments were completed for varying lengths at the optimized concentration of 0.3M sodium bisulfite. As expected, the current density is very similar. It is expected because the plot represents the activity at the working GCE electrode, thus, modifying the counter electrode's length should not affect its activity. Figure 27 reflects the behavior observed at the counter electrode. The trend in which a more negative potential is observed with decreasing length applies. It is also noticed that the amplitudes of the oscillations increase as the length decreases. This is further evidence that the corresponding length and concentration dictates how large the

oscillations can be created as the length of the counter electrode needs to be able to accommodate the difference in current density.

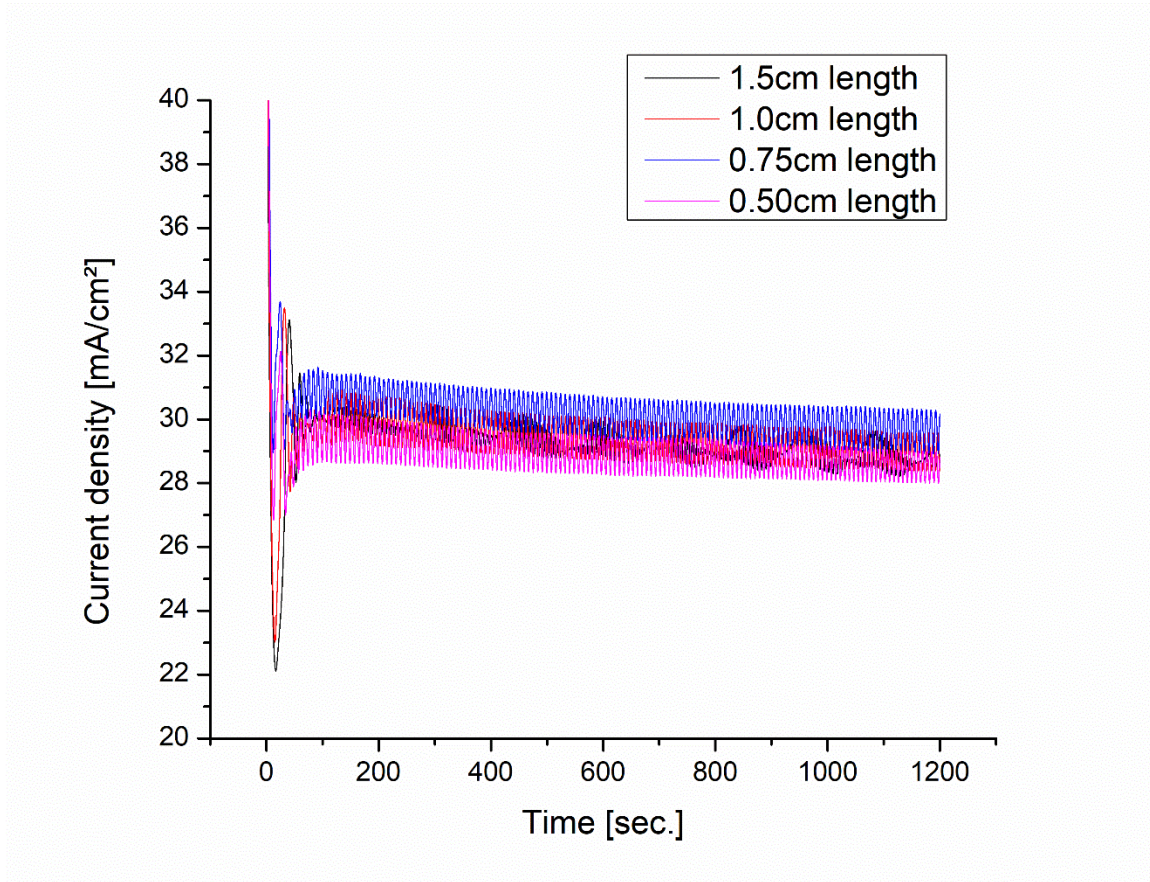


**Figure 26:** Potentiostatic time series of the fabrication of the modified counter electrode in 0.3M sodium bisulfite concentration and 0.1M sulfuric acid concentration varying lengths.

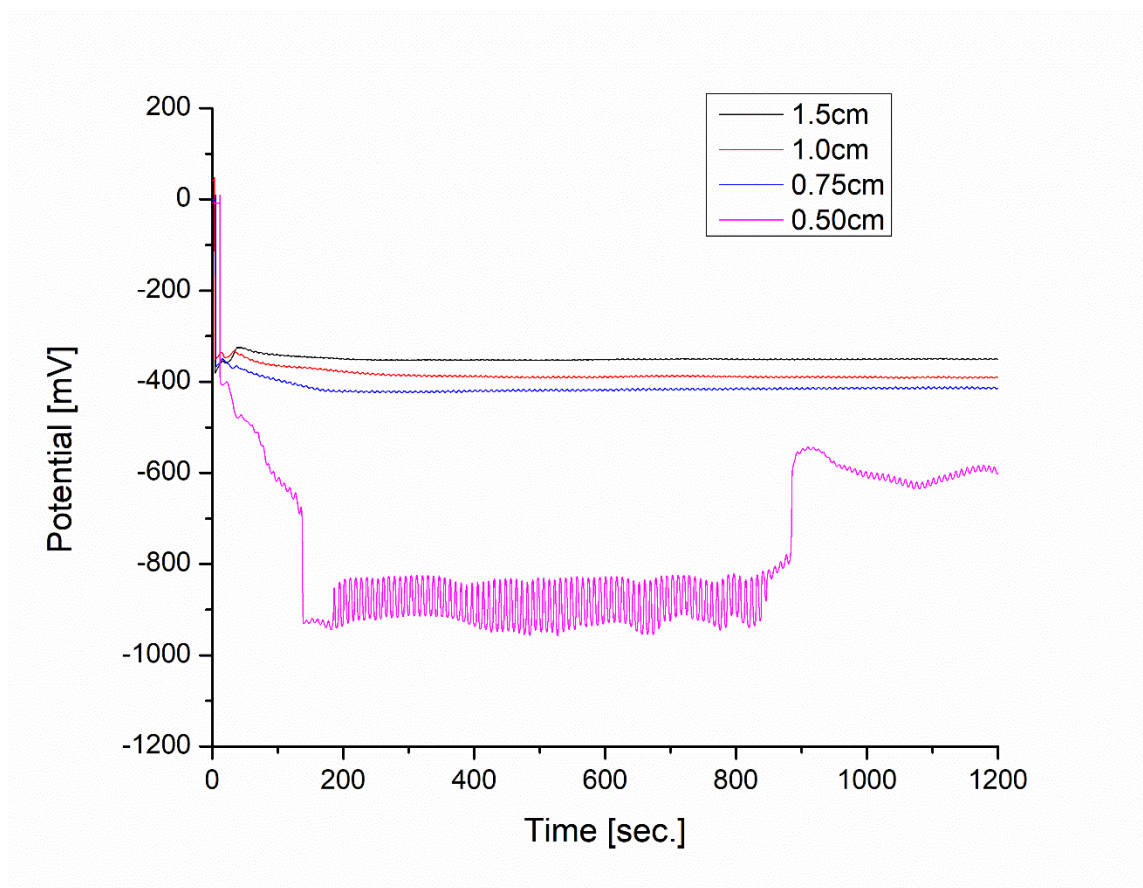


**Figure 27:** Time series of the potential of the counter electrode recorded during the fabrication of a CuS nanoparticles in 0.3M sodium bisulfite concentration.

Figure 28 shows the detection properties of the modified counter electrodes fabricated at various lengths. The CVs were conducted in 0.5mM glucose and 0.1M sodium hydroxide. Each modified counter electrode was utilized as the working electrode and was restricted to a length of 0.5cm. It can be determined that 0.75cm is the optimal length for the best performance in detection based on the anodic peak present at around 400mV followed by 1.0cm, 0.5cm and 1.5cm lengths.

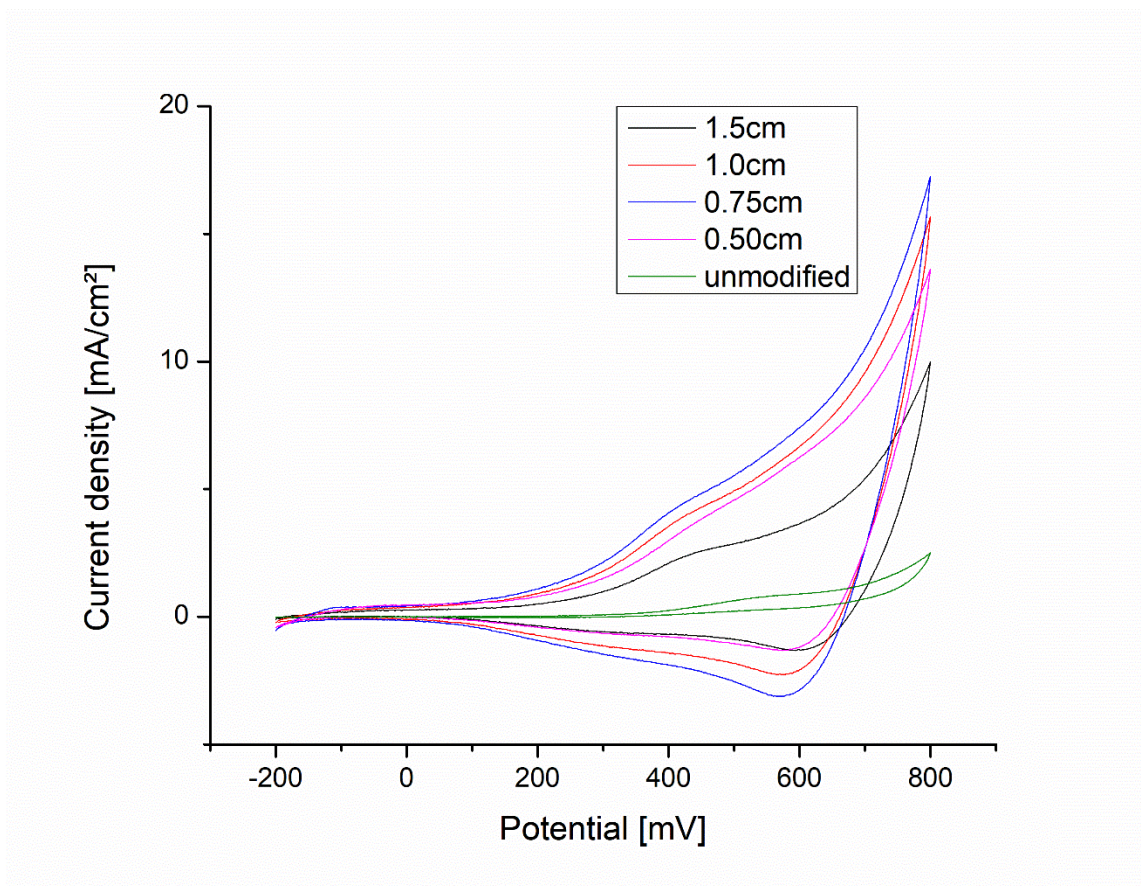


**Figure 28:** CVs of the 10th scan of the modified counter electrodes that were fabricated at varying lengths.

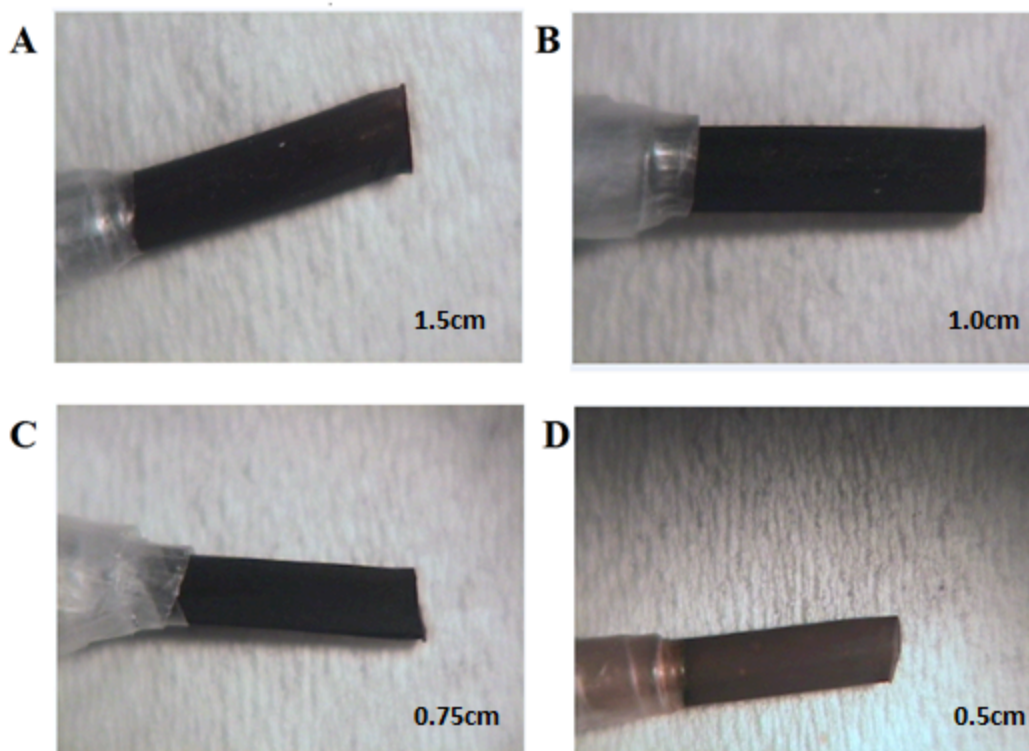


**Figure 29:** Images of the modified copper sulfide electrodes of Figure 26 and 27. A is 1.5cm, B is 1.0cm, C is 0.75cm, and D is 0.50cm. Each modified electrode was restricted to a length of 0.50cm following the fabrication.

Figure 29 shows photos of the copper wires covered with copper sulfide deposits. Careful examination of these images provide the first hand evidence that the copper wire with the 0.75cm and 1.0cm lengths are coated more uniformly and thoroughly in contrast to the ones with the 0.5cm and 1.5cm lengths. Such a difference can be understood based on the variation of the expected current density at the counter electrode. When its area is too small, in order to meet the total current generated at the working electrode, more reactions will take place at the counter electrode, which potentially forced the reduction of hydrogen ions. The formation of hydrogen gas bubbles will physically prevent the deposit from forming on the counter. The formation of bubbles has been observed at the counter electrode with a shorter length. On the opposite end, when the counter electrode

is too long, the same amounts of deposit, which is determined by the activity at the working electrode, will be distributed over a larger area, resulting in a thinner or non-uniform layer.

### 3.4 Detection of D-(+)-Glucose

Glucose was utilized as the analyte in detection in order to optimize the fabrication process. In this section, the oxidation peaks in glucose are further investigated along with its qualitative detection, quantitative detection, and stability analysis.

#### 3.4.1 Qualitative and Quantitative Detection

In order to qualitatively detect glucose with the modified copper sulfide electrode, it is important to determine whether the modified electrode can provide an electrochemical response during a CV which differs from a bare copper electrode. The difference is observable as an anodic and/or cathodic peak in the CV that are absent in the bare copper electrode. Such an observation highlights the electrocatalytic activity of copper sulfide in the oxidation of glucose. In addition, it is important to also compare the modified copper sulfide electrode and bare copper electrode in blank solution with no analyte to ensure that the peaks are not resulting from the electrolyte solution.

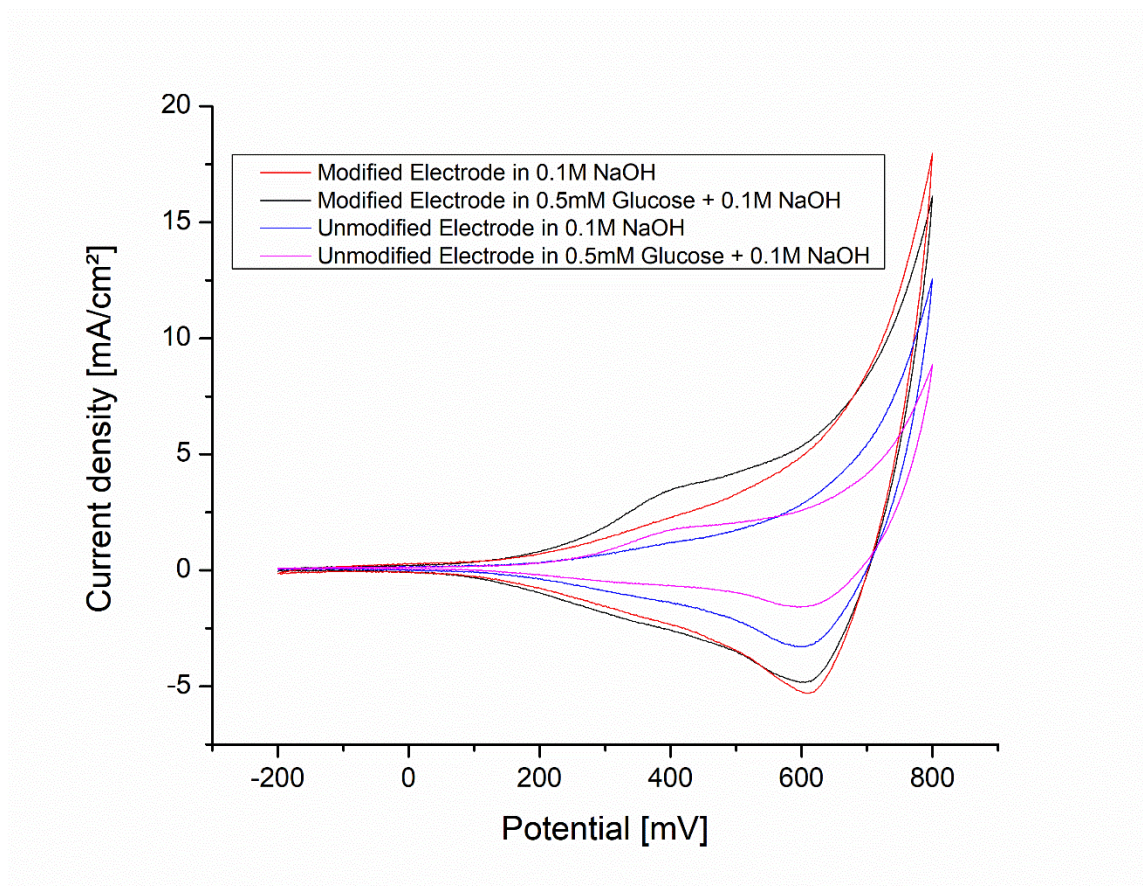


**Figure 30:** CVs of the 10th scan for the modified and unmodified copper electrodes.

As per Figure 30, the modified copper sulfide electrode displays a noticeable anodic peak at a potential of around 400mV in the presence of glucose that is absent in the modified copper sulfide electrode in only NaOH solution (blank). This validates that glucose is detected in solution. In comparison to the unmodified copper wire in a 0.5mM glucose and 0.1M NaOH solution which exhibits a smaller peak, the modified copper wire demonstrates enhancement of glucose detection. This observation is consistent with earlier reports on the high sensitivity of copper sulfide materials to glucose.<sup>36,39</sup>

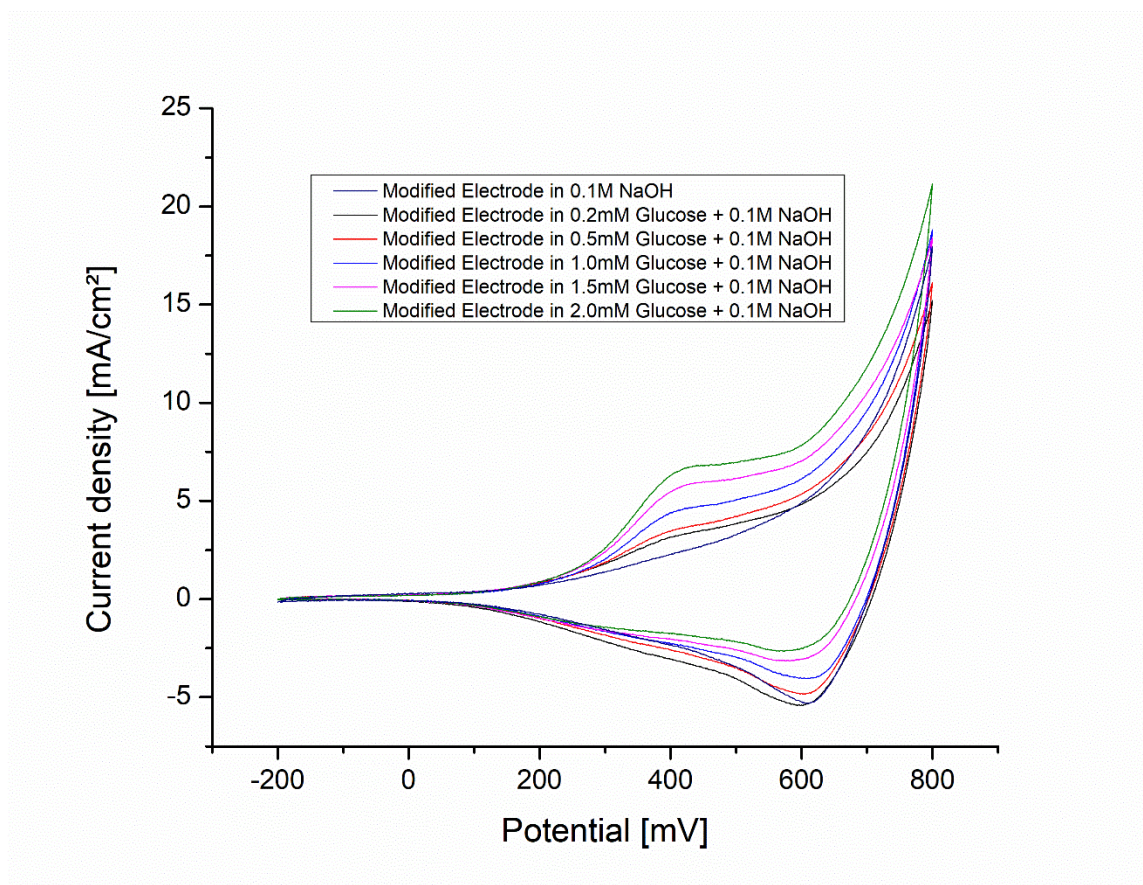


**Figure 31:** CVs of the 10th scan for the modified electrodes in increasing glucose concentration with a scan rate of 100mV/sec. Each electrode was restricted to a length of 1.0cm.

As per Figure 31, a series of CVs were obtained for increasing glucose concentration in 0.1M NaOH supporting electrolyte solution. It is noticeable that the anodic peak in the forward scan is observable at 400mV. The peak's amplitude increases as the concentration increases. It can be observed that glucose can be detected at 0.2mM glucose concentration indicating the sensitivity of the modified copper sulfide electrode. The anodic peak of glucose, however, is significantly lower and less defined at 0.2mM, which indicates that it is close to its limit of detection (LOD). Utilizing the data obtained from the series of CVs, quantitative analysis can be completed. The linear range of the modified electrode is the range of concentrations in which the peak current is a first order

linear function that is dependent on the concentration of the analyte of interest. A calibration curve was constructed in order to determine the linear range of glucose by plotting the peak current during CV as a function of the concentration of glucose in solution.

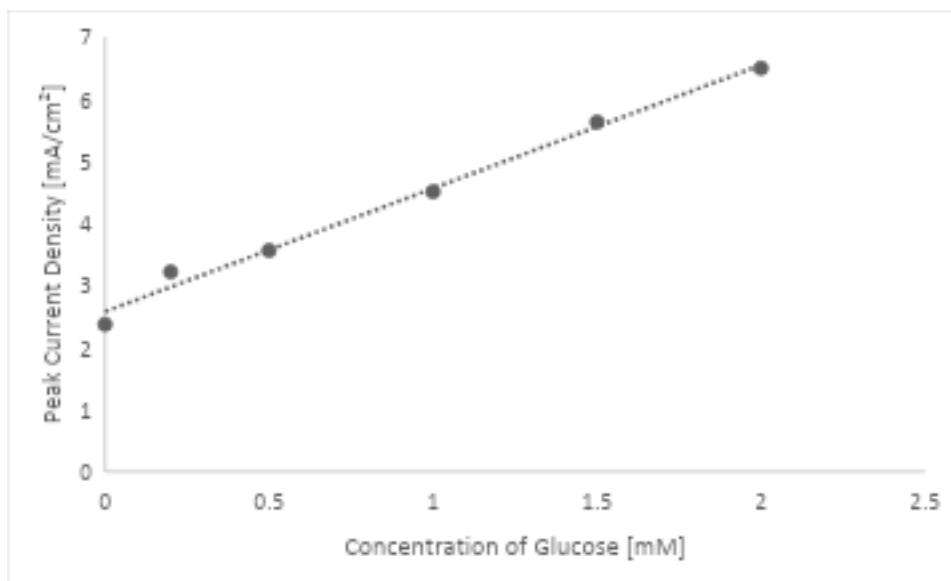


**Figure 32:** Calibration curve of the peak current plotted as a function of the concentration in glucose (mM) during CV using the modified copper sulfide electrode. Data taken from the CVs of the 10th scan for the modified electrodes in increasing glucose concentration.

As per Figure 32, the calibration curve of glucose yields an  $R^2$  value of 0.9907 from the concentration range of 0mM to 2mM. This  $R^2$  value indicates that the peak current of glucose during the series of CV is a first order function that is dependent on the concentration of glucose.

### 3.4.2 Mechanism of Glucose Oxidation

The electrochemical oxidation of glucose occurring on the modified copper sulfide electrode can be characterized as either kinetic controlled or diffusion controlled. A kinetic controlled reaction occurs when the current peak response is predominantly dependent on the rate of charge transfer occurring at the electrode/electrolyte interface. In a diffusion controlled process, the current peak response is determined by the amount of analytic species in solution. Within an unstirred solution, mass transportation to the surface of the electrode occurs via diffusion.

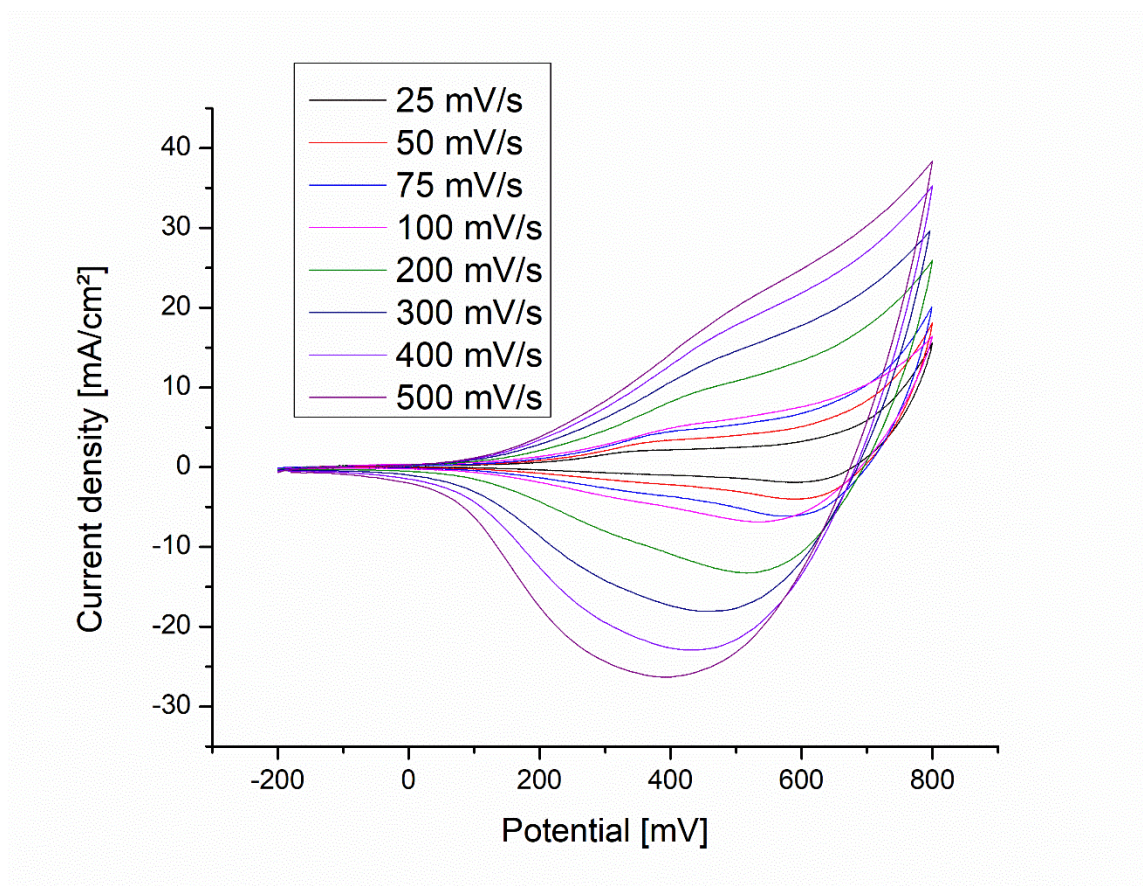


**Figure 33:** A series of CVs at different scan rates. The solution contains 0.5mM glucose and 0.1M NaOH. The modified copper sulfide electrode was fabricated in 0.3M sodium bisulfite and 0.1M sulfuric acid solution for 1200 seconds with a length of 1.0cm.

In cyclic voltammetry, the current passing through the electrode is limited by the diffusion of the species to the electrode surface. The diffusion is influenced by the concentration gradient near the electrode. This concentration gradient is affected by the concentration of species at the electrode and the rate at which the species can diffuse through solution. Changing the cell voltage results in the change in the concentration of the species at the electrode surface as set by the Nernst equation. A faster voltage sweep causes a larger concentration gradient near the electrode, thus, resulting in a higher current. As per Figure 33, the current density increases with respect to the scan rate. Such a correlation can be explained by the Randles-Sevcik equation [7] which is utilized to describe the effect of the scan rate on the peak current and to determine the diffusion coefficient of the electroactive species.<sup>40</sup>

$$i_p = 268600 n^{3/2} AD^{1/2} Cv^{1/2} [7]$$

As shown in equation [7], the peak current in amperes,  $i_p$ , can be calculated where  $n$  is the number of electrons transferred in the redox reaction,  $A$  is the electrode area in  $\text{cm}^2$ ,  $D$  is the diffusion coefficient in  $\text{cm}^2/\text{s}$ ,  $C$  is the concentration in  $\text{mol}/\text{cm}^3$ , and  $v$  is the scan rate in  $\text{V}/\text{s}$ . The peak current can be plotted as a function of the square root of the scan rate to determine the limiting mechanism of the reaction process.

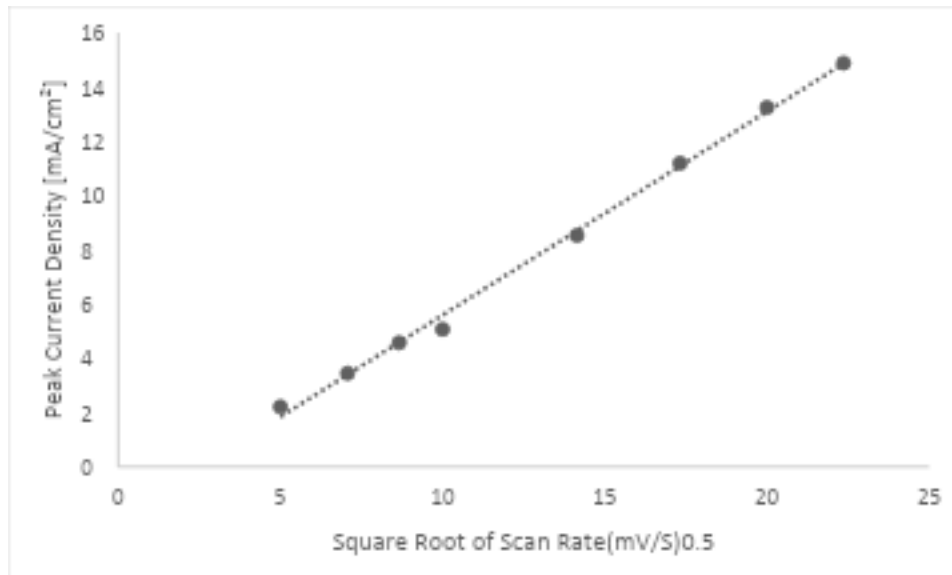


**Figure 34:** Peak current plotted as a function of the square root of the scan rate. The reactions were conducted in a 0.5mM glucose and 0.1M NaOH solution.

As per Figure 34, the experimental plot of the peak current as a function of the square root of scan rate yields a straight line with a linear correlation coefficient  $R^2$  of 0.997. This linear relationship suggests that the electrochemical oxidation of glucose at the modified copper sulfide electrode follows the Randles-Sevcik equation. Therefore, the electrochemical reaction can be classified as diffusion controlled. The  $R^2$  value obtained when plotting the peak current as a function of scan rate is 0.9821, thus, the electrochemical reaction is not kinetic controlled. It is advantageous to have a diffusion controlled mechanism as the peak current is dependent on the concentration of the species of interest, rather than the rate of the reaction occurring on the surface of the electrode. Thus, it provides better quantitative results and applications over a modified electrode that is controlled by its kinetics.

### 3.4.3 Stability

Stability is an important aspect of an electrochemical sensor in regards to the reproduction of consistent results. It is desirable for a sensor to be stable after being stored for long periods of time. In order to determine the stability of the above modified copper sulfide electrodes, these electrodes were stored in air and their performance in the detection of glucose was examined every day for a period of eight days. Specifically, at 24 hour intervals, 10 cycles of cyclic voltammetry in a 0.5mM glucose and 0.1M NaOH solution was completed. After the measurement, the modified electrodes were rinsed with ddH<sub>2</sub>O and were stored in a drawer.

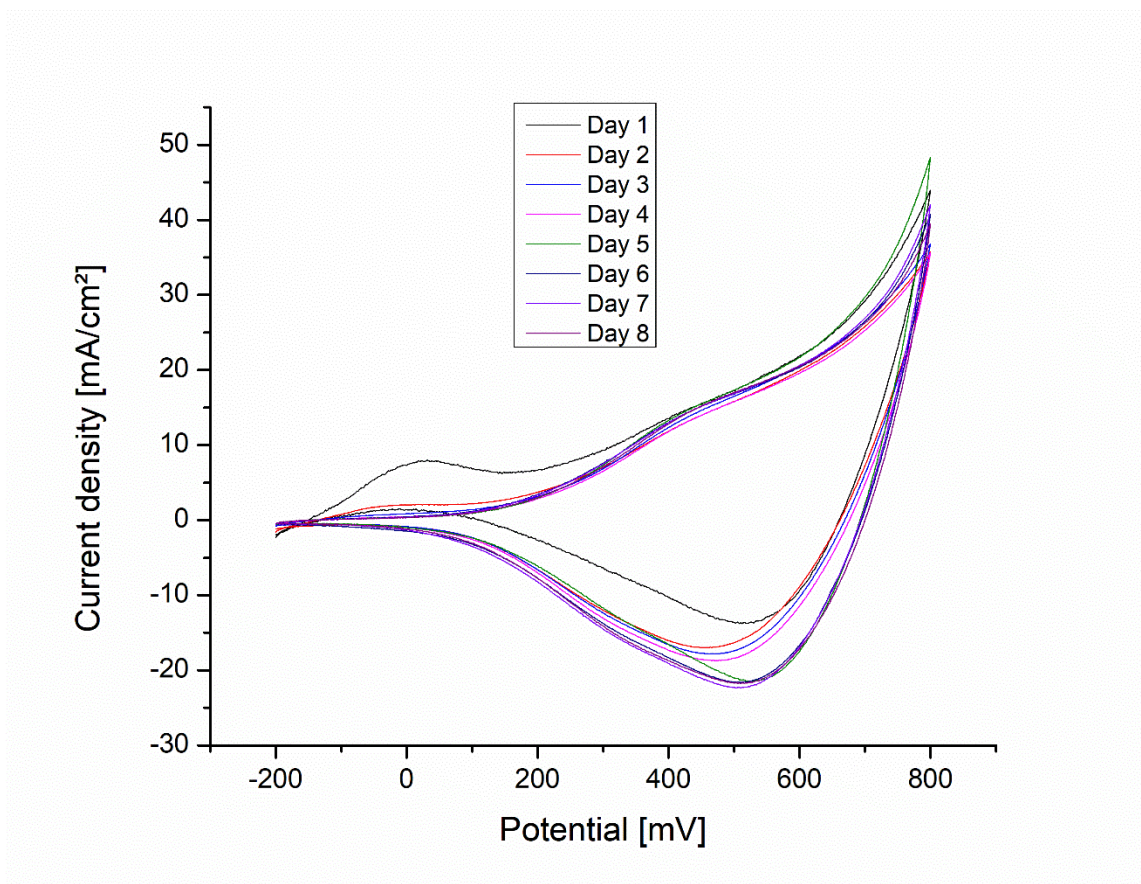


**Figure 35:** A series of CVs of a modified copper sulfide electrode that were fabricated in 0.3M sodium bisulfite and 0.1M sulfuric acid with a length of 1.0cm at 1500mV potential for 1200 seconds.

Figure 35 shows the stability observed in a time span of eight days in which the modified copper sulfide electrode was fabricated and stored in air. The results show that the cyclic voltammograms overlay with each other very well, where the anodic glucose peak in the forward scan at around 400mV is nearly unchanged. Thus, it can be concluded that the electrode coated with copper sulfide nanoparticles is very stable in this eight day time span.

## Chapter 4: Conclusions

A novel electrochemical approach was developed to prepare copper sulfide nanoparticles. The fabrication process occurred at the counter copper electrode during the oscillatory oxidation of bisulfite at a GCE working electrode with an Ag/AgCl reference. Our investigation illustrates that the morphology and size of copper sulfide deposits can be readily manipulated by adjusting the length of the copper electrode, showing the versatility of this electrochemical method. With regards to electrochemical detection of glucose, it was found that copper sulfide prepared at an applied potential of 1500 mV for 1200 seconds and a length of 0.75cm in a solution of 0.3M sodium bisulfite and 0.1M sulfuric acid has the highest activity.

During the fabrication process, the formation of the copper sulfide deposit and oscillatory behavior were observed simultaneously. Whether or not there exists a close correlation between the oscillatory pattern and the particle morphology remains to be explored. The time series of the potential value at the counter electrode allows us to gain some insights into the activity occurring at the counter electrode. Based on the potential obtained, it can be proposed that the reduction of sulfite to S and then to  $S^{2-}$  occurs at the counter electrode. Under such a potential value, the presence of sulfide further facilitates the oxidation of copper resulting in the formation of copper sulfide nanoparticles. In other words, at the counter electrode, two processes occur simultaneously, which consist of the reduction of  $SO_2$  to  $S^{2-}$  and the oxidation of Cu to  $Cu^{2+}$ . The  $S^{2-}$  is predicted to surround the counter electrode and catalyze the reaction resulting in the formation of Cu(II)S.

The modified copper sulfide electrode showed stronger activity towards the electrochemical oxidation of glucose over the copper, as demonstrated with cyclic

voltammetry with an anodic peak at around 400mV in the forward scan. Preliminary characterization indicates that the oxidation of glucose at the modified copper sulfide electrode is likely diffusion controlled.

Scanning electron microscopy measurements validated that at each different set of conditions such as concentration or length, a different morphology was present. The morphology, thus, can be related to its glucose detection properties. The performance of the modified copper sulfide electrodes remains nearly unchanged after 8 days, suggesting that it has great stability and potential for future electroanalytical research.

## **Chapter 5: Future Directions**

Further experiments should be done to construct an overview of the varying parameters in order to optimize the detection properties. As only individual conditions were studied in each parameter while the rest of the conditions were held constant, a systematic investigation in varying more than one parameter is required. Further investigation to determine that the deposit is copper (II) sulfide will be necessary with x-ray photoelectron spectroscopy in order to validate the proposed mechanism. Future in-depth stability analysis would be beneficial to determine the longest time span possible for storage of the modified electrode. A more thorough investigation into the limit of detection of the modified copper sulfide electrode is also necessary in order to determine the lowest concentration of glucose that it will be able to detect. Additional SEM imaging to gain further insight into the relationship of the properties associated each different morphology are also beneficial experiments. The determination of the type of oscillator exhibited are future experiments that would be applicable to the further understanding of non-linear phenomena in electrochemical systems.

## References

- (1) Antuña-Jiménez, D.; Díaz-Díaz, G.; Blanco-López, M. C.; Lobo-Castañón, M. J.; Miranda-Ordieres, A. J.; Tuñón-Blanco, P. *Molecularly Imprinted Electrochemical Sensors: Past, Present, and Future*; **2012**.
- (2) Hu, X. The Development of Polymer-Coated Electrodes for Chemical Detection The Development of Polymer-Coated Electrodes for Chemical Detection, University of Windsor, **2014**.
- (3) Stradiotto, N. R.; Yamanaka, H.; Zanoni, M. V. B. Electrochemical Sensors: A Powerful Tool in Analytical Chemistry. *J. Braz. Chem. Soc.* **2003**, *14*, 159–173.
- (4) Zhang, J. X. J., H. K. Electrical Transducers: Electrochemical Sensors and Semiconductor Molecular Sensors. *Mol. Sensors Nanodevices* **2014**, 169–232.
- (5) Blasco, A. J.; Escarpa, A. Electrochemical Detection in Capillary Electrophoresis on Microchips. *Comprehensive Analytical Chemistry*. **2005**, 703–758.
- (6) Kissinger, P.; Heineman, W. Cyclic Voltammetry. *J. Chem. Educ.* **1983**, 702.
- (7) Elgrishi, N.; Rountree, K. J.; McCarthy, B. D.; Rountree, E. S.; Eisenhart, T. T.; Dempsey, J. L. A Practical Beginner's Guide to Cyclic Voltammetry. *J. Chem. Educ.* **2018**, *95*, 197–206.
- (8) Hnaïen, M.; Lagarde, F.; Jaffrezic-Renault, N. A Rapid and Sensitive Alcohol Oxidase/Catalase Conductometric Biosensor for Alcohol Determination. *Talanta* **2010**, *81*, 222–227.
- (9) Wang, J. Electrochemical Detection for Microscale Analytical Systems: A Review. *Elsevier* **2002**, *56*, 223–231.
- (10) Yuan, H.; Kong, L.; Li, T.; Zhang, Q. A Review of Transition Metal Chalcogenide/Graphene Nanocomposites for Energy Storage and Conversion. *Chinese Chem. Lett.* **2017**, *28*, 2180–2194.
- (11) Hoffman, D. C. Chemistry of the Heaviest Elements. *Radiochim. Acta* **1996**, *72*, 1–6.
- (12) V, E. S. P. B.; Jellinek, F. Transition Metal Chalcogenides. Relationship between Chemical Composition, Crystal Structure and Physical Properties. *Elsevier* **1988**, *5*, 323–339.
- (13) Xia, C.; Li, J. Recent Advances in Optoelectronic Properties and Applications of Two-Dimensional Metal Chalcogenides. *J. Semicond.* **2016**, *37*.
- (14) Theerthagiri, J.; Karuppusamy, K.; Durai, G.; Rana, A.; Arunachalam, P.; Sangeetha, K.; Kuppasami, P.; Kim, H.-S. Recent Advances in Metal Chalcogenides (MX; X = S, Se) Nanostructures for Electrochemical Supercapacitor Applications: A Brief Review. *Nanomaterials* **2018**, *8*, 256.
- (15) Xu, W.; Zhu, S.; Liang, Y.; Li, Z.; Cui, Z.; Yang, X.; Inoue, A. Nanoporous CuS with Excellent Photocatalytic Property. *Sci. Rep.* **2015**, *5*, 1–11.

- (16) Goel, S.; Chen, F.; Cai, W. Synthesis and Biomedical Applications of Copper Sulfide Nanoparticles: From Sensors to Theranostics. *Small* **2014**, *10*, 631–645.
- (17) Ghezelbash, A.; Korgel, B. A. Nickel Sulfide and Copper Sulfide Nanocrystal Synthesis and Polymorphism. *Langmuir* **2005**, *21*, 9451–9456.
- (18) Huang, K. J.; Zhang, J. Z.; Fan, Y. One-Step Solvothermal Synthesis of Different Morphologies CuS Nanosheets Compared as Supercapacitor Electrode Materials. *J. Alloys Compd.* **2015**, *625*, 158–163.
- (19) Wu, C.; Shi, J. Bin; Chen, C. J.; Chen, Y. C.; Lin, Y. T.; Wu, P. F.; Wei, S. Y. Synthesis and Optical Properties of CuS Nanowires Fabricated by Electrodeposition with Anodic Alumina Membrane. *Mater. Lett.* **2008**, *62*, 1074–1077.
- (20) Rao, B. G.; Mukherjee, D.; Reddy, B. M. *Nanostructures for Novel Therapy*; Elsevier Inc., **2017**.
- (21) Malik, M. A.; Wani, M. Y.; Hashim, M. A. Microemulsion Method: A Novel Route to Synthesize Organic and Inorganic Nanomaterials. 1st Nano Update. *Arab. J. Chem.* **2012**, *5*, 397–417.
- (22) Saji, V. S., Cook, R. M. Corrosion Protection and Control Using Nanomaterials. *Elsevier* **2012**.
- (23) Basile, F.; Benito, P.; Fornasari, G.; Monti, M.; Scavetta, E.; Tonelli, D.; Vaccari, A. *A Novel Electrochemical Route for the Catalytic Coating of Metallic Supports*; Elsevier Masson SAS, **2010**; Vol. 175.
- (24) Degn, H. Theory of Electrochemical Oscillations. *Trans. Faraday Soc.* **1968**, *64*, 1348–1358.
- (25) T. M. Koper, M. Non-Linear Phenomena in Electrochemical Systems. *J. Chem. Soc. Faraday Trans.* **1998**, *94*, 1369–1378.
- (26) Christoph, J.; Eiswirth, M. Theory of Electrochemical Pattern Formation. *Chaos* **2002**, *12*, 215–230.
- (27) Orlik, M. *Self-Organization in Electrochemical Systems I*; 2012.
- (28) Atkins, P. W., Paula, J. D. *Atkins' Physical Chemistry (8th Edition)*, 8th ed.; Oxford University Press, **2006**.
- (29) Bell, J. G. Nonlinear Instabilities in Chemical and Electrochemical Systems, University of Windsor, **2017**.
- (30) Sagués, F.; Epstein, I. R. Nonlinear Chemical Dynamics. *Dalt. Trans.* **2015**, 1201–1217.
- (31) White, R. E. *Modern Aspects of Electrochemistry*, 3rd ed.; Butterworths, **1964**.
- (32) Zensen, C.; Schönleber, K.; Kemeth, F.; Krischer, K. A Capacitance Mediated Positive Differential Resistance Oscillator Model for Electrochemical Systems

- Involving a Surface Layer. *J. Phys. Chem. C* **2014**, *118*, 24407–24414.
- (33) Strasser, P.; Eisch, M.; Koper, M. T. M. Mechanistic Classification of Electrochemical Oscillators - An Operational Experimental Strategy. *J. Electroanal. Chem.* **1999**, *478*, 50–66.
- (34) Bell, J. G.; Wang, J. Current and Potential Oscillations during the Electro-Oxidation of Bromide Ions. *J. Electroanal. Chem.* **2015**, *754*, 133–137.
- (35) Pourbeyram, S.; Mehdizadeh, K. Nonenzymatic Glucose Sensor Based on Disposable Pencil Graphite Electrode Modified by Copper Nanoparticles. *J. Food Drug Anal.* **2016**, *24*, 894–902.
- (36) Myung, Y.; Jang, D. M.; Cho, Y. J.; Kim, H. S.; Park, J.; Kim, J. U.; Choi, Y.; Lee, C. J. Nonenzymatic Amperometric Glucose Sensing of Platinum, Copper Sulfide, and Tin Oxide Nanoparticle-Carbon Nanotube Hybrid Nanostructures. *J. Phys. Chem. C* **2009**, *113*, 1251–1259.
- (37) Harris, D. *Quantitative Chemical Analysis*, 7th ed.; Craig Bleyster, **2017**.
- (38) O'Brien, R. N., Rosenfield, C. A., Kinoshita, K., Yakymyshyn, W. F., Leja, J. The Dependence of Concentration Gradient on Current Density at Working Electrodes. *Can. J. Chem.* **1965**, *43*, 3304–3310.
- (39) Kusior, A. Copper Sulfide Materials for Nonenzymatic Glucose Detection. *2018 15th Int. Sci. Conf. Optoelectron. Electron. Sensors, COE 2018* **2018**, 1–4.
- (40) Zanello, P. *Inorganic Electrochemistry: Theory, Practice and Application*; Royal Society of Chemistry, **2003**.

### **Vita Auctoris**

Benjamin Cheung is currently a candidate for a B.Sc. [H] Degree in Biochemistry at the University of Windsor and hopes to graduate in Spring 2019.